REPUBLIC OF TÜRKİYE

ALTINBAŞ UNIVERSITY

Institute of Graduate Studies

Electrical and Computer Engineering

GEOMETRIC ANALYSIS OF PATHOLOGICAL CHANGES IN BRAIN USING MRI IMAGES FOR TUMOR DIAGNOSIS

Aynoor Sameer Mahmood AKMAKCHI

Master's Thesis

Supervisor

Asst. Prof. Dr. Mesut ÇEVİK

Istanbul, 2022

GEOMETRIC ANALYSIS OF PATHOLOGICAL CHANGES IN BRAIN USING MRI IMAGES FOR TUMOR DIAGNOSIS

Aynoor Sameer Mahmood AKMAKCHI

Electrical and Computer Engineering

Master's Thesis

ALTINBAŞ UNIVERSITY

2022

The thesis titled GEOMETRIC ANALYSIS OF PATHOLOGICAL CHANGES IN BRAIN USING MRI IMAGES FOR TUMOR DIAGNOSIS prepared by AYNOOR SAMEER MAHMOOD AKMAKCHI and submitted on 13 /12/ 2022 has been **accepted unanimously** for the degree of Master of Science in Electrical and Computer Engineering.

____

Asst. Prof. Dr. Mesut ÇEVİK

the Supervisor

Thesis Defense Committee Members:

Asst. Prof. Dr. Mesut ÇEVİK	Department of Electrical and Electronic Engineering, Altınbaş University	___________________
Asst. Prof. Dr. Timur İNAN	Department of Software Engineering, Altınbaş University	___________________
Asst. Prof. Dr. Hatice ÇOBAN	Department of Software Engineering, Doğuş University	___________________

I hereby declare that this thesis meets all format and submission requirements of a Master's thesis.

Submission date of the thesis to Institute of Graduate Studies: ___/___/___

I hereby declare that all information/data presented in this graduation project has been obtained in full accordance with academic rules and ethical conduct. I also declare all unoriginal materials and conclusions have been cited in the text and all references mentioned in the Reference List have been cited in the text, and vice versa as required by the abovementioned rules and conduct.

Aynoor Sameer Mahmood AKMAKCHI

Signature

DEDICATION

To the spirit of my parents, with pride.

PREFACE

To begin, I want to express my gratitude to God for blessing me with the perseverance and fortitude necessary to complete this assignment. Finally, I'd want to express my deep gratitude to my supervisor, Asst. Prof. Dr. Mesut ÇEVİK, for all of his guidance, patience, inspiration, and depth of knowledge over the duration of this research. I've learned a lot about independence thanks to his guidance as I've spent many hours doing research for my thesis. I want the best for him in anything he does. Also, I appreciate the feedback and assistance from the remainder of my thesis committee. The radiologists at Kirkuk Hospital, together with the professors and doctors who provided invaluable assistance in developing the study and datasets, have my deepest appreciation. I could not have finished the research without their help, which was crucial. I appreciate everyone who has cheered me on and helped me financially while I worked toward my goal of obtaining a college degree. Finally, I'd want to express my gratitude to the Master's students and staff who have been so encouraging to me while I worked on my thesis.

ABSTRACT

GEOMETRIC ANALYSIS OF PATHOLOGICAL CHANGES IN THE BRAIN USING MRI IMAGES FOR TUMOR DIAGNOSIS

Akmakchi, Aynoor Sameer Mahmood

M.Sc., Electrical and Computer Engineering, Altınbaş University,

Supervisor: Asst. Prof. Dr. Mesut ÇEVİK

Date: 12/2022

Pages: 78

Any kind of camouflage treatment increases the chance of developing a brain tumor diagnosis analysis or another condition. Researchers have found common risk factors and symptoms of brain tumors after poring through massive amounts of data from individuals who have been diagnosed with the disease. New therapeutic approaches are being developed all hours of the day and night thanks to advances in scientific technology. The doctor may discover and diagnose a brain tumor by looking at this photograph. Consciousness loss is a major risk factor for the development of brain tumor diagnosis (Segmentation, measurements, detection, and classification), and this trend is only expected to grow. This study utilizes an algorithm to forecast disease risk specifics based on the detected tumor region in brain MRI scans and measurements, and the work focuses on determining the tumor's range and form. A tumor is an abnormal, uncontrolled development of tissue. There are several tumor varieties, each with its own unique characteristics and therapeutic approaches. Due to the nature of the tumor and the small size of the cerebral cavity, brain tumors are very dangerous and potentially fatal (space formed inside the skull). According to studies of causes of death, brain tumor deaths are disproportionately high in wealthy nations.

It accurately forecasts disease details from the tumor location and establishes the stage and size of the tumor. Segmentation techniques for brain tumors are the combination of fuzzy c-means and thresholding used here. This technique enables tumor tissue segmentation with precision and consistency on par with that hand segmentation. To insure the medical report, we have done a color map of the brain tumor and non-infected area. When testing the proposed framework on MRI and CT images, the tumor identification rate was about 96%, with a DSC of 97 % and an IoU of 96 for automated and manual brain tumor segmentation.

Keywords: MRI Images, Machine Learning, Segmentation and Measurements, Classification, Brain Tumor.

TABLE OF CONTENTS

Pages

LIST OF TABLES

Pages

LIST OF FIGURES

Pages

ABBREVIATIONS

MRI	:	Magnetic Resonance Imaging
PCA	:	Principal Component Analysis
FNN	:	Feed-Forward Neural Network
KNN	:	K-Nearest Neighbor
RT	:	Ripple Transform
BFC	:	Bayesian Fuzzy Clustering
ROI	:	Region Of Interest
WPTE	:	Wavelet Packet Tallies Entropy
JOA	:	Jaya Optimization Algorithm
DAE	:	Deep Auto Encoder
FCM	:	Fuzzy C-Means
DOPS	:	Darwinian Optimization of Particle Swarm
CT	:	Computed Tomography
PET	:	Positron Emission Tomography
TE	:	Transmission Interval
GM	:	Gray Matter
WM	:	White Matter
PVE	:	Partial Volume Impact
LDA	:	Linear Discriminant Analysis

SMO : Sequential Minimal Optimization

DPOS : Darwinian Optimization of Particle Swarm

CAD : Computer-Assisted Diagnosis

HOG : Histogram Of Oriented Gradients

LBP : Local Binary Pattern

CNN : Convolution Neural Network

SVM : Support Vector Machine

SSIM : Structured Similarity Index Comes

MSE : Mean Square Error

PSNR : Peak Signal To Noise Ratio

PCD : Pixels Corrected Detected

PND : Pixels Not Detected

PFPR : Probability False Positive Results

MS : Merit Score

IOU : Intersection Over Union

DSC : Dice Similarity Coefficient

1. INTRODUCTION

As a result of aberrant cell growth, a tumor is formed in the body. Since the brain is the body's master controller and regulator, malignancies, which are masses of tissue generated when aberrant cells grow out of control, are the most critical organs to study. Brain cancer has yet to be linked to a single cause. Malignant brain tumors, despite their rarity, have a significant mortality rate since they are located in the body's most essential organ (just 2.0 percent of all documented malignancies in the globe). As a result, early and correct segmentation of brain tumors is critical to reducing the death toll. An MRI scan is a time-consuming and labor-intensive technique. The human body's various anatomical components may be revealed through image processing methods. Simple imaging technologies can't reveal the human brain's abnormal structure. Magnetic resonance imaging (MRI) allows for the differentiation and clarification of the human brain's neural architecture. Start by focusing on noise reduction and color visualization of the tumor area in order to reduce the complexity of the segmentation and measurements of tumor size, location, and shape variation. After segmentation, morphological filtering may be used to remove any noise. A tumor's benignity or malignancy may be determined with high precision segmentation as well.

1.1 CLINICAL BACKGROUND AND REVIEW

It is possible to obtain images of various parts of the body for the specific purpose of diagnosis and treatment by making use of medical imaging techniques and the technology that is made available through digital health. In addition to other soft tissues, a three-dimensional image of the brain and spinal cord can be obtained through the use of the magnetic resonance imaging (MRI) method. This approach is frequently utilized when depicting human anatomy and function [5].

Because it is in charge of coordinating all the functions carried out by the body, the human brain is widely regarded as one of the most significant components of the human organism. Infections, strokes, and tumors are just a few of the many conditions that can lead to brain damage. There are also many other conditions that can cause brain damage. A brain tumor is a mass of abnormal cell improvement that can either be cancerous or noncancerous and that develops in the brain. Brain tumors can be either benign or malignant. When it comes to determining whether or not a patient has a brain tumor, the most reliable diagnostic tool is an MRI (MRI). In recent years, there has been an uptick in [6] interest in the field of medical image processing, specifically in regards to MRI images. This is because there is a requirement for a thorough, unbiased, and effective investigation of significant amounts of data. Medical research and clinical assessments of the diseased and healthy human mind are dependent on the identification of brain malignancies and the automated categorization of brain tissue from MRI images. Without this information, neither medical research nor clinical assessments will be possible. This is true regardless of the state of the person's mental health. The step in the process of medical imaging in which different regions of an MRI picture are sliced off and grouped together in order to prepare for further computation is the most essential step in the procedure.

This study gives a broad overview of brain tumors as well as the diagnostic tests that may be used to locate them. Also covered are the potential causes of brain tumors. The physical foundations upon which MRI technology is built are another topic that will be covered in this chapter. This article presents a thorough analysis of the dataset, as well as its acquisition and application from the perspective of traditional MRI. In addition, regardless of the fact that the primary goal of this thesis is to segment brain tumors, the approaches and methods developed would be applied to the other clustering challenging task of brain damage in to demonstrate their capacity to segment an image. This will take place despite the fact that the primary objective of this thesis is to segment brain tumors. In spite of the fact that the primary objective of this thesis is to segment brain tumors, this will still take place. [7] This article presents a summary of the pathogenesis of ischemic stroke, as well as its prevalence in the general population.

Principal Component Analysis (PCA) and a two-dimensional Deep Wavelet Transform (D-DWT) are two types of methods that can be used in order to determine which facets of a picture are the most significant. Both of these methods can be found in the field of image analysis (PCA). They used a Feed-forward Neural Network (FNN) in conjunction with a K-Nearest Neighbor (KNN) method in order to categorize the data (KNN). Ripple Transform (RT) model was developed by Das et al. [9] by applying the Least Squares Support Vector Machine classifier to the task of feature classification. When diagnosing tumors, a fluid vector and T1 weighted images may both be helpful diagnostic tools. [10]. the diffusion coefficients were incorporated into the diffusion tensor images [11] so that the tumor could be located. Researchers studying brain tumors have had a difficult time identifying and eliminating the characteristic that stands out as being the most significant because the number of potential traits is always expanding, making it difficult for them to do so. Additionally, it may be challenging to select training and testing samples that will provide satisfactory results [12, 13]. This method of categorizing MR brains was initially developed by Amin et al. [14], who were the pioneers in this field. After using a Gaussian filter to reduce the amount of noise in the images of the brain, the following processing steps were carried out: embedding, cyclic, contrast, and block appearance were recovered for segmentation processing, and a technique called cross-validation was used for classification. When Chen et al. demonstrated fuzzy clustering with Markov random fields, the fuzzy clustering membership of the initial image was incorporated into the Markov random field function. This allowed the researchers to produce more accurate results. The utilization of segmented supporting data in conjunction with a hybrid strategy results in a significant improvement in the effectiveness of this method.

Raja et al. [16] were successful in the identification of brain cancers by using a hybrid deep auto-encoder and Bayesian Fuzzy Clustering (BFC)-based segmentation. They began the process of eliminating noise by using a non-local mean filter as a pre-processing step on the data. This was the first stage in the procedure. One of the approaches that they used was called Bayesian fuzzy clustering, and it was employed in the process of separating the brain tumor. BFC was one of the procedures. After the segmentation process was complete, they recovered important characteristics by using a broad variety of methods in addition to information theory metrics, the Scattering Transform (ST), and the Wavelet Packet Tallies Entropy (WPTE) (WPT). A JOA (Jaya Optimization Algorithm) was paired with a soft-max regression approach in order to produce an accurate description of the location of the brain tumor. This was done in order to provide an accurate diagnosis. In addition to that, we made use of a DAE (Deep Auto Encoder). After the data from the BRATS 2015 database had been imported into their models, they next proceeded to run their models.

Arunkumar et al. [17] proposed the concept that an automated system may be utilized to not only identify brain cancers but also discriminate between the many subtypes of tumors that can occur in the brain. The preliminary identification of malignant tumors utilizing MR data needed only the most minute of characteristics, and at no time was the participation of a human being necessary in any way, shape, or form. The process of splitting brain tumors might be improved in three distinct ways, and each one of these techniques is described below. They began by using K-means clustering as their basis for classification in order to separate the various sections of the district. During that time period, K-means clustering was widely used as a primary concept for organizing MR data. Second, as a direct result of the training procedure, ANN was used in the process of choosing the correct item. By the time the mitotic stage was reached, all of the features of the tissue that were linked to a cancer diagnosis had been eradicated. Grayscale features might be used as an assist in making the distinction between benign and malignant brain tumors. The SVM's inquiry into the segmentation and brain identification upwards into using their model in order to carry out the essential task. This allows the SVM to complete the research. The accuracy of their model comes in at 94%, while its sensitivity sits at 90%, and its specificity is at 96%. They claim that their model is 94% accurate.

Through their study, Mekhmukh and his colleagues came to the conclusion that the best possible results could be accomplished by using PSO in combination with outlier rejection and a level set [18]. [Citation needed] When conducting the process of segmentation of MR brain tumors, it is standard procedure to make use of the fuzzy c-means method. The membership function in a normal implementation does not take any information about the surrounding region into consideration, nor does it take any external variables into consideration. Neither of these things should be the case. The approach could be especially vulnerable to image noise and unevenness, and the degree to which it is susceptible to these difficulties varies depending on how the centroid is originally set. However, the method might be particularly susceptible to picture noise and unevenness. The authors created extensive FCM picture segmentation in order to boost the external suppression of standard FCM clustering algorithms and limit the algorithm's susceptibility to noise. This was accomplished via the use of extensive FCM image segmentation. This was accomplished through the use of extensive FCM image segmentation.

The development of in-depth FCM image segmentation was the key to achieving this goal. The FCM method employs cluster centers that have been chosen at random, in contrast to the PSO algorithm, which gives considerable thought to the selection of its cluster centers. In addition to this, their software takes into account the information regarding the neighborhood's demographics as well as its physical layout. It turned out that their strategy was successful. Figure 1.1 demonstrates that all of the works of art included in this section have segmented a tumor inside the brain, rather than at its boundary. This is demonstrated by the fact that the tumor is segmented.

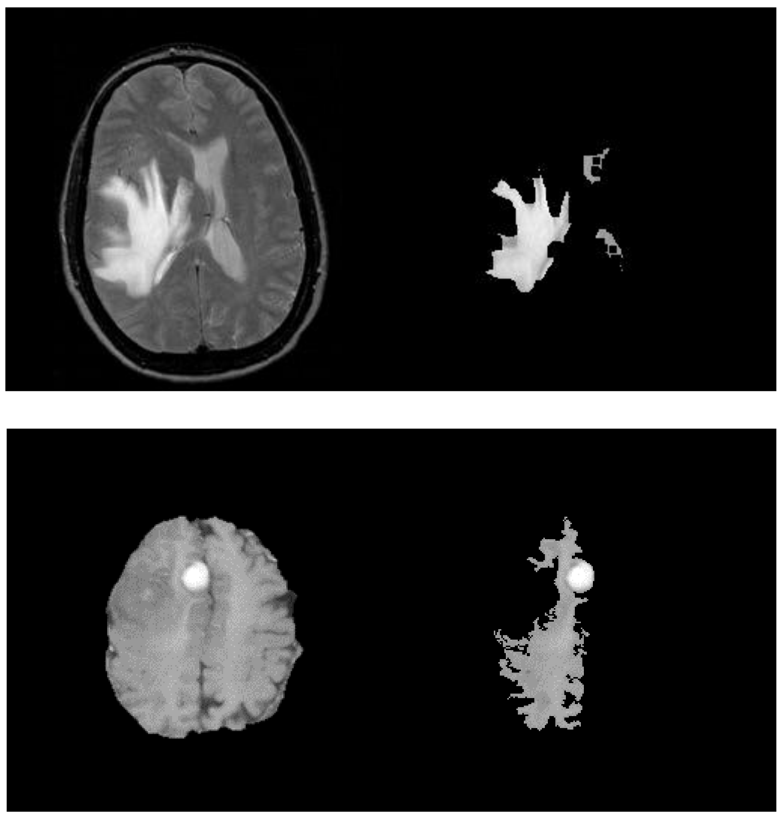

Figure 1.1: Examples of the different developed method.

Figure 1.2 shows an example of how difficult it is to segment a brain tumor when it is on the brain's outer edge, a problem that our approach resolves. There's a problem here that researchers and professionals have a hard time with, and we're trying to figure out how to fix it in our way.

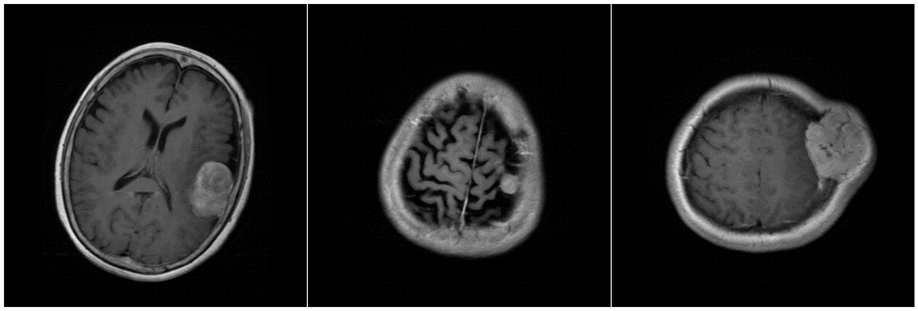

Figure 1.2: Example of difficult tumour segmentation located on the end of tumour.

1.2 PROBLEM DEFINITION

Brain tumors affect an estimated 60,000 individuals in Europe and 18,000 people are diagnosed each year. According to the National Health Service [1,] there is reason for concern over the rising incidence of brain tumors in the United Kingdom. Gliomas are the most common kind of brain tumor, accounting for around 82% of all brain and normal brain tumors [2]. The results of this research highlight the need of giving careful consideration to the treatment of cancer of this kind. Despite the fact that there are a great deal of distinct varieties of brain tumors, primary brain tumors are quite rare. It is very uncommon for cancers to start in the brain or nervous system and then spread to other regions of the body. The great majority of brain tumors, on the other hand, originate in other parts of the body and then make their way to the brain through the circulatory system or the lymphatic system. These tumors are not considered primary tumors.

The tumor's size, cell type, and stage all have a role in how well it reacts to treatment. Tumor segmentation is thus essential for surgical and other treatment planning. It is possible to utilize medical imaging to detect and assess malignancies. For a range of clinical disorders, deciding on the optimal course of action in order to support surgery and schedule radiotherapy An precise measurement of the tumor's 3D volume may be achieved by drawing a circle around the tumor's target area manually. It takes less time to segment a tumor using semi-automatic procedures. Manual segmentation is more susceptible to human mistakes since people have a limited ability to recognize visual characteristics in a picture. When working with huge MRI datasets, accurate segmentation and identification is always a good idea.

i. Our research focuses on the laborious process of automating the segmentation of brain tumors as well as the measurement of the tip of the brain.

ii. MRI scans are often used to investigate the structure of the human brain.

iii. Using the information from the MRI scan, our method intends to first identify the presence of a tumor and then determine the extent of that tumor in the brain.

iv. It is anticipated that the procedure will improve the current screening methodology for brain tumors and, by minimizing the need for further treatments, might possibly cut the costs associated with receiving medical care.

v. There is a significant amount of processing that has to take place before biological imaging data can be correctly characterized and interpreted.

1.3 MOTIVATION

It is remarkable how many distinct kinds of cells can be found in a single human body. It is possible for a tumor to form if the development of a cell is not correctly handled, which might lead to its creation. Imaging techniques such as computed tomography (CT) and magnetic resonance imaging (MRI) scans are used in the process of detecting tumors. Utilizing a variety of technologies such as medical image processing, machine learning, and computer vision, the purpose of this research is to reliably detect and classify different types of brain cancers. Specifically, we are focusing on gliomas, which are a subtype of primary brain tumors. It's possible that neurosurgeons, radiologists, and other specialists in the medical field may gain something useful by using this method. The simulation software tool Mathematica, which is the industry standard, will be used in order to increase the diagnostic sensitivity, specificity, and accuracy of screening for brain tumors. Mathematica is now the gold standard in the field. This gadget might potentially decrease the number of necessary follow-up scans by improving the procedures that are currently in place, which would result in a reduction in the overall cost of delivering medical care. In order to appropriately classify and understand the data that is produced from biological imaging, it is required to apply a broad variety of processing techniques.

This initiative was developed in order to provide assistance to members of the medical community, namely radiologists, who are engaged in the non-invasive and low-cost diagnosis of brain cancer. In the realm of medical image analysis, the use of computer-assisted treatments is becoming an increasingly frequent practice. The segmentation of distinct tissues or organs is a factor that plays an enormously significant role in the process of making medical judgments, such as those addressing the evaluation of risks and the categorization of diseases. The results of the segmentation process contribute to the processes of analysis, diagnosis, and planned therapy. Correct segmentation may be helpful in identifying brain tumors and planning treatment since it provides a rapid and objective estimate for the volume of the tumor. This estimate may be used in the diagnostic process. Brain tumors continue to be a focus of study, despite the significant amount of time and effort that has previously been committed in the field.

1.4 AIM AND OBJECTIVES

The purpose of this thesis is to create an automated image processing system that is able to appropriately segment and categorize brain tumor and sub-tumor tissue produced from multimodal MR data. This system will be developed as part of this thesis. The process presently relies on human labor and takes a significant amount of time.

The following goals will need to be fulfilled before this one can be checked off the list: Investigate different feature representations for accurate brain tumor segmentation and size measurements, preferably ones that combine machine-learned features with handcrafted features. The former addresses the issue of local dependencies, and the latter addresses the issue of the handcrafted features (which offer global information). Investigate the method that is most efficient for combining the features obtained from multi-modal MR scans, while at the same time eliciting the greatest amount of helpful information from each unique MR modality. Develop an automated way for constructing a tumor segment that agrees with the delineation conducted by experts across all grades of glioma. This may be accomplished by making use of a single MRI methodology that is applied by a large number of institutions. Following the extraction of features from a segmented tumor and the subsequent categorization of the tumor, the application of machine learning for classification may then take place.

1.5 ORGANIZATION OF THESIS

Thesis has five chapters. This chapter presents brain tumors, their diagnostics (segmentation, measurement, cancer prediction), and brain assessment techniques. This part includes the problem statement and thesis aims. Chapter 2 focuses on the literature review and newest relevant research. Machine learning algorithms and computer vision methodologies address Chapter 3's segmentation and measurement procedures in detail. Chapter 4 presents experiment results evaluating computer vision segmentation and machine learning for cancer prediction. Chapter 5 summarized the results and recommended additional investigation.

2. LITERATURE REVIEW AND BACKGROUND

The human nervous system is responsible for a number of activities, one of which is the dissection and categorization of brain tumors [19]. The hypothalamus is the part of the brain that regulates a wide range of bodily activities, including cognition, movement, and breathing, transmission, and heart rate [20]. Since tumors are characterized by the expansion of malignant growth, they have the potential to be a primary cause of increased mortality not only in adults but also in infants. This is because of the fact that cancerous development is what defines a tumor. There is a possibility of finding tumors in or close to the brain. Both primary and secondary tumors are available for examination to identify whether or not they are cancerous [21]. Primary tumors are more likely to be malignant. Computed tomography (CT), magnetic resonance imaging (MRI), and x-ray imaging (X-Ray) are all examples of imaging methods that may be used to evaluate the structure of the brain and locate malignant growths [22–24]. [25–27] More and more doctors are turning to magnetic resonance imaging, sometimes known as MRI, while trying to diagnose patients with brain cancer. This strategy is used by the computer vision brain tumor segmentation technology [28] to break up an image into its component pieces. The strategy involves splitting the surrounding pixels of the picture into a set of predetermined characteristics or qualities for each pixel. It is important to note that this technique is also known as pixel separation.

In the field of medical imaging, the primary objective is to retrieve pertinent information and rectify object data with the smallest amount of inaccuracy as is humanly feasible. Error correction is really essential for a number of reasons, and this is one of them. In the field of medical image analysis, the first step that must be taken is to obtain the image in a state where it can be processed. At this point, the image is prepared for the upcoming phase of post-processing by executing a range of activities. These jobs include filtering and the removal of noise [29].

The improvement of pictures for use in medical applications is made possible by the use of preprocessing software. This may be performed by altering the characteristics of the image in order to enhance its aesthetic attributes [30]. The deployment of separation operators as well as morphological operators is part of the second phase. They are the ones that are accountable for identifying how big the tumor is as well as where it is located [31]. In the realm of image processing, segmentation is an extremely important procedure that is an essential component in the process of gleaning information from intricate medical scans. This information might be used in the process of diagnosing and treating patients. The fundamental purpose of image segmentation is to split up a digital picture into different sections that cannot be joined with one another [32]. Note: image segmentation is also known as image dissection. [33] The technique of segmenting a picture may be carried out in a number of distinct ways. Techniques of segmentation include the region-based segmentation and the edge detection segmentation that uses clustering algorithms. These are only two examples of segmentation methods. Following the processing and segmentation of medical scans, feature extractions are required in order to distinguish malignancies based on the particular intensity strength or texture pattern that they present [34]. Brain tumors [35] are categorized by radiologists according to whether or not they have a homogenous or heterogeneous texture. Because of this, they are able to discern between the many forms of cancer. These observable traits give us with recommendations for how to construct a Computer-Aided Diagnosis (CAD) that is able to assess whether or not a person has brain cancer [36].

2.1 VARIOUS CATEGORIES OF MEDICAL PHOTOGRAPHS

[37] Some examples of medical images that use a variety of imaging techniques include CT, MRI, and chest x-rays (CXR). Other examples of medical images that use a variety of imaging techniques include Positron Emission Tomography (PET) and Nuclear Magnetic Resonance Imaging (NMR). However, owing to the massive number of data generated by this method, effective quantitative evaluations can only be used in clinical practice under very particular circumstances [38]. This is because this method generates such a large amount of data. In most cases, computed tomography imaging is favored over magnetic resonance imaging because to its wider availability, cheaper cost, and improved early-stock sensitivity. CT gives the facts essential to make accurate judgements in the overwhelming majority of different types of situations. Images of a hemorrhage demonstrate a startlingly hyper-density that stands in stark contrast to its surroundings [39]. Imaging using X-rays has had a significant impact on both the

cognitive and functional structure of the field of medical research. The kind of radiation known as X-rays are responsible for the emission of electromagnetic waves. If we compare it to employing microwaves and light, we may say that it is similar. CXR is used to generate a two-dimensional picture by traveling through the body. This gives you an idea of what is happening on the inside of your body. Different components of the body are shown in a range of grayscale and monochrome tones. This is because different organs absorb radiation at differing intensities, as is discussed in more detail in [40]. In addition, the magnetic resonance imaging (MRI) scan provides information on a broad variety of bodily structures, which is information that can only be obtained with the assistance of an X-ray [41].

2.2 CONCEPTS IN ADDITION TO TERMINOLOGY

By clarifying important terminology and ideas, this section makes both the issue and its solution far more clear. Photos of brain tumors are essential for local researchers, who need to be able to detect, assess, and interpret the pictures they find.

2.3 WHAT KIND OF TUMOR IS THIS?

There are many different types of tumors, and some of them may develop in the nervous system, particularly in the brain or other areas of the nervous system. Some of these tumors can even spread to other regions of the body. As a direct result of this, we refer to this particular region of the brain as an abnormality or an aberrant.

There is a substantial degree of confluence between the characteristics of tumors and those of cancerous growths. A mass of abnormal tissues that may or may not contain fluid is referred to as a tumor. Tumors may occur in almost any part of the body. Neoplasm is another word that may be used to refer to cancer. It is possible to classify tumors as primary or secondary, depending on the kind of cancer that has formed in the patient. This distinction may be made. The cells from this organ are incorporated into the mass that will develop into the tumor. The nervous system provides a natural source of fuel for early tumors, which enables the slow development of early tumors. This is because the nervous system is located in the brain and spinal cord. [42] Gliomas are a specific kind of brain tumor that are often discovered in the central nervous system. Gliomas are distinguishable from other types of brain tumors by the presence of glass cells, which serve as the primary component of the tumor's architecture.

The unchecked growth of aberrant tissues in the brain may be detrimental to the healthy cells that are found in the regions that surround them. It appears like this new development is a cancerous growth. The three principal types of cancerous growths are noncancerous, malignant, and premalignant tumors. Benign tumors make up the majority of all cancerous growths. Benign is used to describe something if it does not have any potentially harmful characteristics or inclinations. The term "malignant" may be used to anything in the body that has been identified as having a cancer diagnosis. It is possible for the signs of a cancer that has not yet reached the malignant stage to indicate the presence of a precancerous characteristic. The cells that join together to form secondary tumors might have originated from a wide range of places all around the human body. It's very likely that news will spread very quickly. To put it another way, the presence of cancer cells is directly responsible for the development of secondary tumors. Therefore, cancer and tumors are not the same thing; rather, tumors represent the earliest stage of malignant cells. Cancerous cells can only form when there is a preexisting healthy cell. The categorization of tumors is based on a wide range of criteria, some of which are included in the following list:

i. The location of the tumor inside the body.

ii. The diagnosis of a malignant tumor in the patient's brain

iii. Your identification must be kept in the secure storage locker.

The kinds of cells that are included inside a tumor are another factor that may be used to classify it.

i. This is a brain tumor that is made up of neurons.

ii. Glial cells make up the bulk of this malignant growth, which is known as a tumor.

iii. A tumor consisting of bacterial and cell bases has grown.

iv. Meningioma’s are one of many different kinds of tumors that may develop in the brain.

These are the pathology-based categories that are most often seen in the United States.

The carcinogenic. The non-cancerous.

It is possible that these scans will reveal malignancies in various parts of the brain, as shown in Figure 2.1.

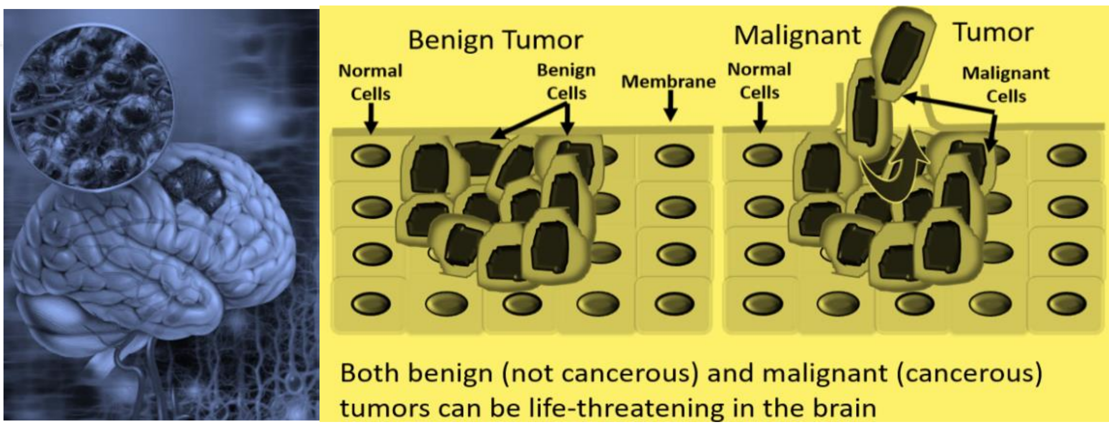

Figure 2.1: An example of a tumour-filled brain scan.

2.4 AN MRI IMAGE SHOWING THE TUMOR'S CHARACTERISTICS

When compared with X-rays, the results that emerge from imaging using an MRI machine are far better [43]. Patients who undergo magnetic resonance imaging, which may be used to diagnose sickness and decide on a course of therapy, are not placed in any danger of being exposed to potentially harmful radiation during the procedure. Pre-processed magnetic resonance imaging have the potential to be used in the process of diagnosing and locating brain cancers [44]. The sort of MRI machine that is used is determined by the specific requirements of the patient, and there are many different kinds of MRI machines that may be used. The T1, T2, and FLAIR sequences are only three examples of the many other kinds of MRI sequences that might be used as inputs for the preprocessing step. It is essential to have an understanding of both the TE and the TR in order to get a comprehensive appreciation for the MRI images that are at your disposal. The length of time that elapses between the transmission of an RF pulse and the reception of an echo signal is referred to as the "Transmission Interval" (TE), and it is denoted by the acronym TE (time of echo). The term "repetition time," which is abbreviated as "TR," refers to the amount of time that elapses between the transmission and receipt of a series of successive pulses. Images of the CSF fluid taken with a T1-weighting [25]. [45] Gray Matter, often known as GM, may be identified by its darker hue in comparison to White Matter (WM). Fat seems to have a brighter appearance on T1 scans, which are ideal for assessing the anatomical makeup of the brain. In order to produce the images, the TE and TR periods need to be as short as 500 milliseconds and 14 seconds, respectively (uses longitudinal relaxation).

Because CSF and fluid have a higher signal intensity than tissue does in T2-weighted imaging [46], they seem brighter than tissue does. This is because tissue has a lower signal intensity. In order to get photos from the T2 telescope, long-exposure timers of TR 4000 milliseconds and TE 19 milliseconds were used (traverse relaxation). T2 is the most appropriate technique to utilize for assessing edematous tissue due to the fact that it is simpler to see in liquid. FLAIR [47] does not need nearly as much cerebrospinal fluid as T2 does, yet it is still able to spot anomalies in a clear and accurate manner. An evaluation of cerebral edema may be accomplished by the use of this particular device. When taking images, both the exposure length and the total exposure time are stretched out to exceedingly long periods (TR-9000 msec, TE-114 msec) a comparison of the two distinct groups of MRI pictures is shown here in Figure 2.2 in a side-by-side format.

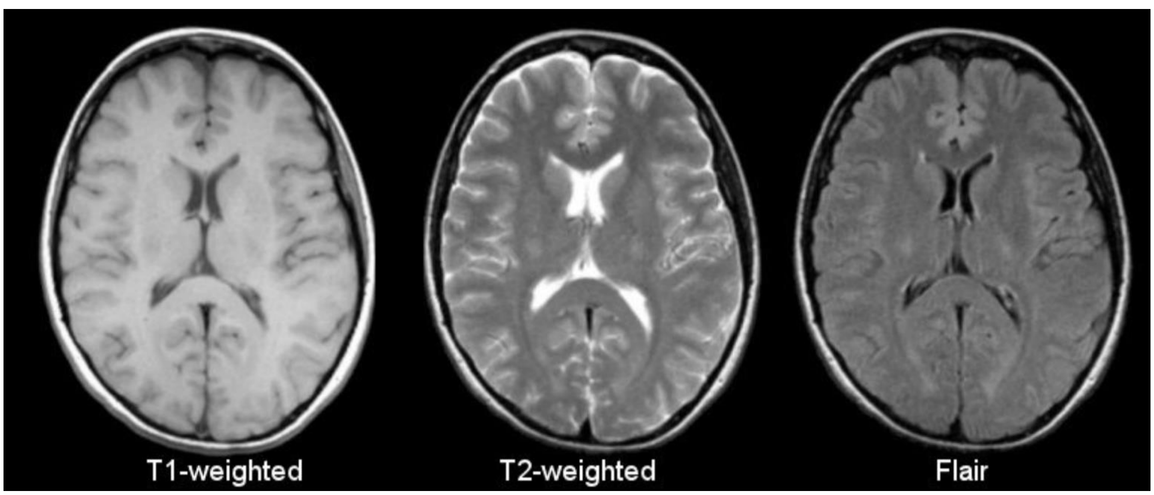

Figure 2.2: Type of MRI imaging technique.

2.5 MEDECAL IMAGE ANALYSIS METHODS

Image processing is required in order to make an accurate diagnosis because of the wide variety of imaging modalities that are currently available. This can be accomplished in a number of different ways; however, the methods that are considered to be the most important for this study are image segmentation and filtering respectively. These primary techniques have the potential to be utilized in the process of accurately detecting cancers in MR images of the brain.

Enhancing medical pictures requires a preprocessing procedure. In this phase, we apply a number of restrictions that might have a negative impact on picture quality. A manual adjustment is part of our preprocessing. An important part of the preprocessing procedure is removing the film and skull sections from brain MR/CT images so that brain tumors may be more readily and securely recognized during post-processing [48]. Before moving on to the next step, which is needed to find brain tumors, the images are first segmented.

Utilizing the MRI images obtained with the flair and diffusion-weighted modalities, methods for inspecting the myocardial infarction lesion are suggested [48]. An example is shown in Figure 2.3 for image processing and analysis.

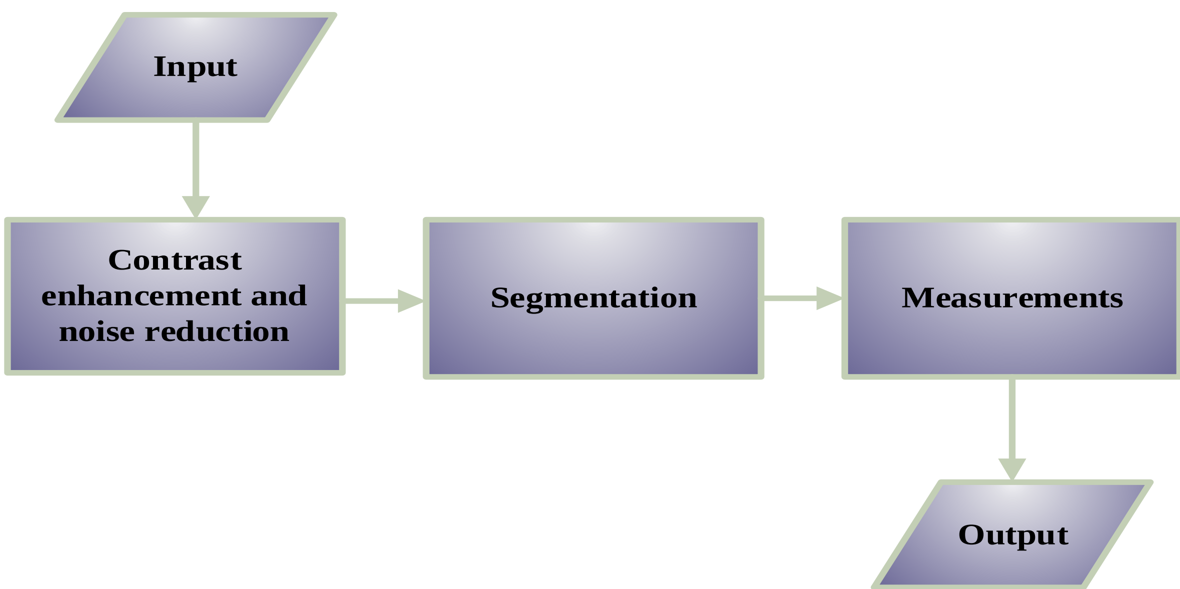

Figure 2.3: Analyzing and interpreting of CT medical images.

2.5.1 Filtering and Noise Reduction

Image processing starts with filtering and de-noising. Several restoration procedures eliminate noise introduced during picture capture, transmission, or compression. This approach improves results by improving picture resolution (See Figure 2.4)

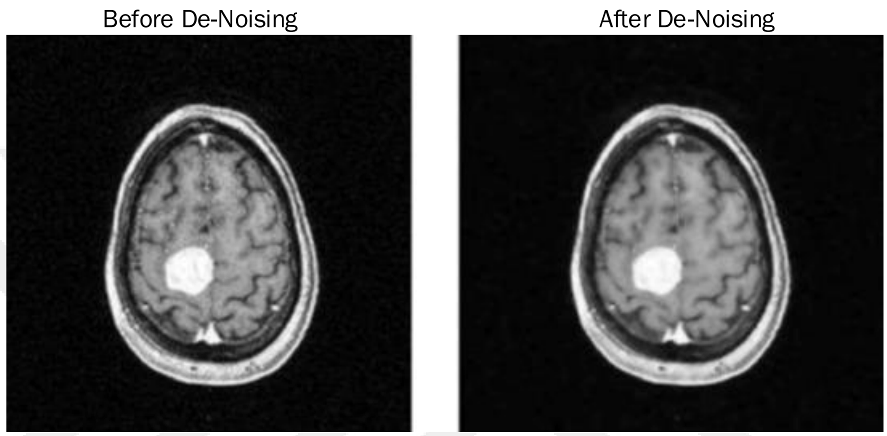

Figure 2.4: Image de-noising is seen in this example.

2.5.2 Image Segmentation

Image processing is essential because of the variety of imaging methods. This may be done in many ways, but this research focuses on filtering and visual segmentation. These approaches can diagnose brain MR cancers. Preprocessing improves medical images. In this step, we implement image-degrading constraints. We preprocess manually. Preprocessing brain MR/CT pictures involves removing film and skull portions so brain cancers may be more easily identified in post-processing [49]. Before finding brain tumors, photos are segmented.

Using flair and diffusion-weighted MRI images, the myocardial infarction lesion is analyzed. Image segmentation is important in medical imaging. After improving brain tumor photos, many segmentation techniques will be used [50]. Clinicians segment brain tumors manually, semi-automatically, and automatically [51–54]. When splitting a picture, color, texture, contrast, and gray level are considered. The technique requires a digital grayscale image. Anomalies are needed for a CT or MRI. Fragmenting an image reveals more about the topic. K-mean clustering and fuzzy c-mean are utilized to generate accurate performance data [51].

A brain tumor is an uncontrolled growth of tissue that damages nerves and other organs. Neuron proliferation or development might induce unwanted cell advancement. Figure 2.5 summarizes.

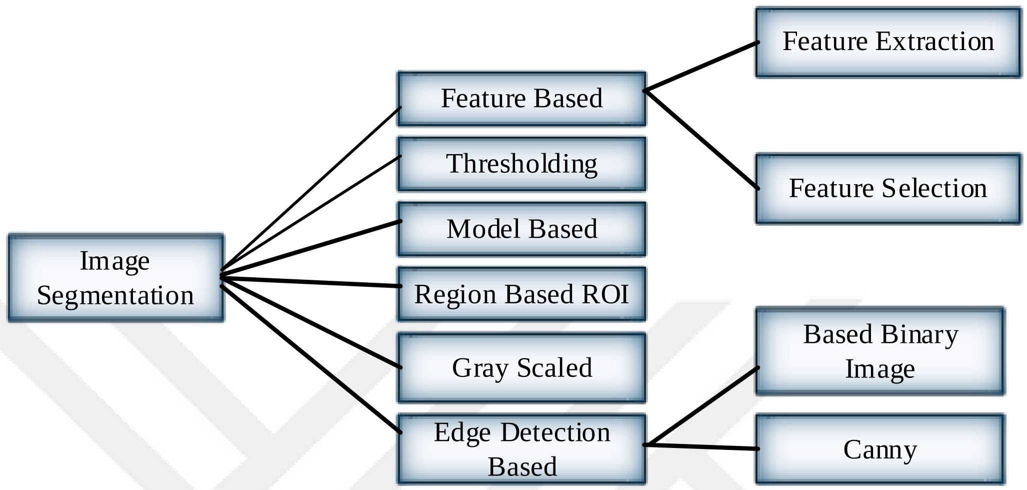

Figure 2.5: Types of image segmentation.

A thorough assessment of the patient's symptoms is required at regular intervals as the evolution of a brain tumor moves forward. When looking for malignancies in the brain, MRI is the imaging method of choice. The removal of a tumor without causing damage to healthy tissue is a very challenging task. The identification of tumors was accomplished by the use of an image processing strategy, which included the capturing, preprocessing, and augmentation of the image in addition to image segmentation and classification [53].

2.5.3 Fuzzy C-Mean

One of the most successful approaches to data clustering is the fuzzy clustering technique (FCM). FCM is an unsupervised method that may be used to a variety of tasks. Some examples of these tasks include factoring, grouping, and segmentation. For instance, it might be used in the building of greenhouses for use in horticulture, as well as in astronomy, biochemistry, image processing, and medical assessment. Within the FCM, there are at least two data zones that are able to manage the Partial Volume Impact (PVE). This is an iterative approach that just looks at how bright the segmented image is [54]. In an iterative search for the most accurate clustering of the data structure that is physically possible, this technique is put to use to look for a series of fuzzy clusters and the cluster centers that are connected with them. Using this approach [55–57], the most recent batch of power points, n, is partitioned into a predetermined number of fuzzy sets. [55–57] In order to produce segmented pictures, these methods are used in conjunction with an FCM algorithm.

By using FCM, you will be provided with an in-depth look at all thirteen of the different FCM segmentation approaches in a one convenient location. The use of FCM segmentation algorithms to brain tumors is going to be the primary focus of this study. The fragmentation of the tumor is an essential stage in the process of diagnosing brain tumors using mechanical means. When compared to other types of image segmentation, brain tumor segmentation is a particularly challenging technique because of the distinct distinctions in the anatomy of the brain. The scans of the brain often have low contrast, which makes this process much more challenging. Early identification of brain tumors is beneficial not only for patients but also for doctors and other medical professionals [57].

2.5.4 Threshold-Based Segmentation

Pattern recognition was created as a result of the relevance of picture segmentation as well as its vital function in the extraction of objects in the field of image processing. This is one of the reasons why. To simplify the process of locating the data that provides the greatest match, identifying the needed area, and extracting it, it essentially separates the input image into several different sections.

The threshold-based segmentation method is the most fundamental approach to the process of segmentation. The image is divided into sections using one or more thresholds, with the number of thresholds used dependent on the density values [58 – 60]. When there are more than two types of areas in a photograph that correspond to different items, a local threshold is used to segment the photograph. Setting a specified threshold value allows for the separation of light objects against a dark background according to the degree of the image's severity. Those pixels in the image that are above the threshold are assigned the value one, while those that are below the threshold are given the value zero. Pixels with a value of one are used to represent the Region of Interest (RoI), whereas pixels with a value of zero are used to represent the background of the image. In the present research project, a threshold-based segmentation model is used. This approach gives us the ability to improve the amount of usable information by experimenting with the input image at a variety of thresholds and Max values. In the first step, the threshold-based categorization splits the grayscale image into two blocks, one black and white and the other white and black. Brain MRI scans performed with varying threshold settings yielded the best possible results. Figure 2.6 [60] provides a description of the method known as Threshold-Based Segmentation.

1. Select the initial value of threshold.
2. Divide the image into sub-blocks of size M × N.
3. For each sub-block, B do
4. Calculate the standard deviation for B.
5. Select the Global threshold as the threshold T that separates an object from the background
6. A Global threshold is applied for B that has a standard deviation greater than one.

Figure 2.6: Threshold-based segmentation.

2.5.5 Review of Medical Image Analysis

In principle, brain cancer classification systems that use deep learning may be broken down into two categories: those that sort brain MRI scans into "normal" and "abnormal," and those that further categorize the latter into a number of different forms of brain cancer. The use of CNNs for brain tumor detection and grading has attracted the attention of scientists as a powerful tool in the disease diagnosis and classification field, which will improve the accuracy of the grading of detected brain tumors and aid doctors in devising optimal treatments, ultimately leading to a higher success rate. For the last several years, researchers in the machine learning area have focused their attention on a new and exciting trend: deep learning. Deep learning is a strong machine-learning approach that has been extensively employed in multiple applications to solve different complicated issues that demand exceptionally high accuracy and sensitivity, especially in the medical industry. One of the most prevalent and severe malignant tumor disorders, a high-grade brain tumor diagnosis results in a relatively short predicted life span. Therefore, classifying a brain tumor soon after diagnosis is crucial for developing an appropriate treatment strategy. Two scenarios were tested in this study to determine how best to assign a tumor grade to brain images: those with clipped tumor lesions, and those with no such restrictions. These examples are MRI scans of brain tumors with T1-Weighted contrast enhancement. An innovative CNN architecture is trained with these pictures to determine network heft. Both compressed and original image images were shown to be very accurate, sensitive, and specific.

An Improved Support Vector Machine (ISVM) classifier has been suggested for use in the context of brain tumor research [66]. SVM is used in the dataset of the proposed technique to identify cancerous aberrant cells in MRI scans. This dataset includes the processed image that has been segmented using the K-mean approach.

The K-mean approach was used to segment the picture, and that result is likewise included in the dataset. The experimental findings that were achieved by utilizing the strategy that was recommended yielded more accurate results than those that were produced by using any of the other available approaches. Because this method has the potential to detect tumors in a fraction of a second, the total amount of time necessary for the treatment will be cut down significantly. Employing k-means clustering, patch-based image processing, item counting, and tumor evaluation, the authors of [67] provided a method for automatically detecting brain malignancies in MRI images. This method was accomplished by using a combination of these four methods. An analysis of twenty real MRI images demonstrates that MRI scans have the capacity to detect malignancies of any size, even those that have very low intensities or scales. This finding was gleaned through the analysis of the images. There is the potential for integrations of robotic surgical technology and automated therapy equipment, both of which are now being considered as viable options. Despite the growth of the tumor as well as fluctuations in both its volume and position, it was proven that an approach to identifying tumors based on MRI is successful.

In [68], it was proposed that a basic way of drawing a border around the tumor may be applied. This suggestion was made in regard to MRI images. It is well knowledge that the traditional KM technique suffers from a variety of limitations, some of which may be alleviated by using the k-mean strategy. The random initialization of centroid clusters and the sensitivity to noise are two of these problems that might be found in this method. Our major objective is to integrate the DPSO method and morphological reconstruction with the KM algorithm. This is the target that we have set for ourselves (MR). As part of the DPSO methodology, patient MRI scans serve as the foundation for the generation of cluster centroids. In addition to this, it may assist in the reduction of background noise and the production of clusters that are simpler to spot.

KM clustering and DPSO-based multilevel thresholding were two of the established segmentation techniques that were used in the evaluation that was conducted in [69] to assess the efficacy of the strategy that was recommended as a means of doing so. These techniques were used to ascertain how well the new tactic was implemented. The successful use of the method that is detailed in this article has made the detection of tumors at an earlier stage far less difficult. A novel approach to separating different parts of MRI medical images is detailed in this paper. This method is different from others since it employs a unique clustering algorithm called K-mean, which integrates images with the most prominent gray level, and it also includes photographs. In this specific instance, the process of picking k randomly chosen pixels in line with the main gray level of the picture was explained. [79] When it came to establishing a high degree of image accuracy, the results of the tests showed that was more effective than the K-Means strategy.

In order to segment brain lesions in MRI and CT images, a hybrid approach that incorporated the median filter and morphological processes was reported in [70]. This technique was used to segment brain lesions. This method was used in order to section off brain lesions. When preprocessing brain pictures, a median filter and k-means fragmentation are used together. This is done in order to limit the amount of impulsive noise in the images. Two of the performance measures that are used to evaluate the effectiveness of a system on well-known datasets are the speed with which the data can be segmented by the automated system that was recommended and the amount of time it takes for the system to actually carry out its functions.

It has a pretty outstanding accuracy rate of 94 percent when compared to manual delineation by an expert radiologist [71], which may be found in the following: The researchers have an interest in studying the process of tumor segmentation. Based on a technique known as fuzzy c-means, which makes use of skull stripping and places an emphasis on the kernel as its initial point of reference. In order to enhance the segmentation algorithm, combining a number of kernels requires data from geographic regions, which may be obtained by collecting the relevant data. We decided to employ global matching information across image distributions rather than information on a pixel-by-pixel basis so that we could cut down on the amount of time spent processing. This was done so that we could save time. A procedure known as co-segmentation, which makes use of the graph cut approach, is performed in order to locate the specific location where the edema and the tumor meet. This is done in order to eliminate the tumor edema. Because the tumor can be seen more clearly in [71], this treatment strategy is the one that ought to be selected as the course of action. The simulations reveal that our technique is superior in terms of separating tumors and edema into the components that make up their wholes as a whole. Specifically, this is done by separating the fluid that makes up the tumors.

The use of fuzzy c-mean classification, which has been utilized in medical image processing systems [72], may be used to identify brain tumors that have been detected by MRI. BCET labels and enhances pictures by making use of a variety of filters, one example of which is a median filter. After the picture has been segmented using the FCM clustering approach, a nimble edge detector is used to generate an edge map of the brain tumor. This step is done after the image has been segmented. The previous stage, which consisted of "segmenting" the picture, is followed by this one. The canny strategy achieves superior results for both BCET and FCM. This is due to the fact that it utilizes ideal input photographs that are of a higher quality and separates these images into uniform pieces. This is due to the fact that it uses high-quality photos as input. As a direct result of this, medical professionals will be delighted with the results, and the overall picture quality is superb.

A noise-free and impact-reduced edge map was the result of implementing the technique that was proposed for reducing the amount of impact and decreasing the amount of noise. [73] Using fuzzy c-means and brain-storm optimization, it is possible to achieve the goal of developing a hybrid better segmentation solution for medical images. This was the goal of the proposed approach. Cluster centers are given priority in the brain-optimization storm in the exact same manner that they would be given priority in any other swarm technique. Although the Brain-Storming Optimization (BSO) has shown some encouraging outcomes, the fuzzy technique calls for a considerable amount of time to elapse before it can provide the optimal network design.

The suggested FBSO was effective, durable, and significantly lowered the optimization algorithm segmentation time in the BRATs dataset. It also had an accuracy of 93 percent, 94 percent, 97 percent, 97 percent, and 95 percent sensitivity in the ideal solution. In addition to this, the FBSO was successful in reducing the total amount of time spent segmenting the data.

A Pre-smooth Non-Local Means filter (PSNLM filter), which is also known as a fuzzy C-means algorithm, is used in order to identify the noise process, as stated in [74]. This is accomplished by combining an FCM method reformulation with PSNLM. Due to the fact that the PIGFCM approach was developed with this prior knowledge in mind, it is able to make effective use of this data. It was shown that this approach is capable of accurately recognizing tumors by decreasing the amount of time needed on image de-noising, improving the precision of segmentation, and preserving a high level of productivity.

According to [75], the process of detecting which regions of the brain have tumors and which regions do not contain tumors utilizes FCM fragmentation as one of the methods. [75] In addition, the multilayer discrete wavelet transform may be used so that wavelet properties can be derived. A DNN is finally being put to use with the goal of effectively identifying tumors that may occur in the brain. KNN, Linear Discriminant Analysis (LDA), and Sequential Minimal Optimization are all methods that are quite similar to these other methods (SMO). Although it has an accuracy rate of 96.97 percent, the DNN-based classification of brain tumors is very challenging and time-consuming to carry out.

Enhanced contrast may be achieved by using adaptive histogram equalization, as shown in [76]. [74, 77] Following this step, an FCM-based separation is used in order to isolate the tumor from the remainder of the picture of the brain. Once the Gabor properties have been retrieved, aberrant cells in the brain are filtered out using the information utilizing the Gabor properties. The KNN fuzzy classification is used at the very last step of the process of determining whether or not brain MRI data contains abnormalities. There is a significant amount of complication. Having said that, there is a significant lack of accuracy. In this specific piece of study, the convolutional neural network was used in order to enable the automated identification of a previously unknown kind of brain tumor.

A strategy was offered for constructing a clear and accurate boundary inside the MRI images around the location of the tumor [77], and it was advised that this boundary be formed utilizing the procedures that are outlined in the following sentence: The conventional technique of knowledge management is plagued with a number of flaws that are remedied by the method that has been suggested. These deficiencies include noise sensitivity based on the k-mean technique as well as random centroid cluster formation. The Darwinian Optimization of Particle Swarm (DPSO) technology, the KM algorithm, and the process of morphological reconstruction are going to be combined into a single operation as a primary goal of this project. Morphological reconstruction is also going to be a primary goal of this project (MR).

In order to accomplish the initialization process of cluster centroids in MRI medical pictures, the DPSO approach is used. This is done in order to improve the efficiency with which the photos may be examined. In addition to this, the MR filter is used so that noise may be eliminated and more concentrated clusters that can be readily differentiated from one another can be produced. It was determined whether or not the proposed method was successful by comparing it to a wide variety of cutting-edge segmentation techniques, such as the conventional KM clustering algorithm and DPSO-based multilevel thresholding. Both of these techniques were used to determine whether or not the proposed method was successful. In order to evaluate how well the new tactic might be implemented, these algorithms were put to use. According to the findings, the method that has been suggested as an alternative for the early detection of malignancies may in fact be practicable.

An approach to the segmentation of medical pictures was created, with a primary emphasis on the use of magnetic resonance imaging (MRI) scans as the primary data source. In contrast to the ways that were first created, the suggested approach makes use of a one-of-a-kind K-mean cluster algorithm that takes into account the gray level that occurs most often in the images. This is in contrast to the methods that were initially established. To provide more clarity, the incorporation of the image is the means by which this strategy achieves the desired result. The subject of arbitrarily selecting k the number of pixels from an image while simultaneously taking into account the overall amount of gray that was there was brought up at some point throughout the course of the discussion. The findings of the tests that were conducted with the method that was suggested revealed that it demonstrates superior performance in terms of picture correctness in comparison to the methodology that is utilized by the traditional K-Means algorithm [66]. The tests were carried out with the method that was suggested.

The purpose of the trials that were carried out was to illustrate [78]. The goal of this presentation was to demonstrate a hybrid strategy for the segmentation of brain lesions. This technique included the use of morphological processes, median filtering, k-mean clustering, and Sobel edge detection in the different imaging modalities of MRI and CT. In addition to that, morphological operations were implemented. After using a crucial pre-processing step known as the median filter, the captured pictures of the brain are then placed through a process known as k-means segmentation in an attempt to get rid of the impulsive noise. The goal is to boost the picture quality by doing this.

Typical datasets are used to measure the effectiveness of the proposed automated system in terms of metrics like segmentation precision and processing speed. For the purpose of gauging the system's efficacy, this evaluation is conducted. By comparing its results to those of manual delineation performed by a seasoned radiologist, the results showed that it achieves a high degree of accuracy in its output, reaching 94%. The fact that it was able to attain this degree of precision is evidence of this. A big step in the right direction has been taken.

The segmentation of tumors and edema would be the primary areas of focus for the study that is intended to be conducted. Skull stripping and a method known as kernel-based fuzzy c-means were the foundational techniques for the development of this approach. Combining a large number of kernels in a manner that is consistent with the geographical information that is presently available has the potential to make the clustering process more efficient. Our method of multilevel segmentation is founded on the information that can be employed to discover global matches across picture distributions. This information forms the foundation of our method, which is founded on this information. Since of this, the process of computing has become less complicated because it is no longer necessary to look for information that can be discovered on a pixel-by-pixel level. In this framework, the Graph cut technique is applied as a co-segmentation in order to determine the exact cut-off point between the edema and the malignancy in order for the edema to be eliminated from the tumor. This is done in order to allow for the removal of the edema from the tumor.

In order to reduce the swelling caused by the tumor, this procedure is carried out. This is done in order to make it possible to drain the fluid that has collected inside of the tumor, which necessitated the procedure. This technique makes it easier to see the edema and generates more space, both of which make it feasible to remove the tumor in the most efficient way possible. These two benefits are key constituents of a successful treatment plan. The results of the simulation indicate that our approach is more effective than the other methods that are presently being used for the completion of tumor and edema segmentation [79].

Hamad et al. (2018) developed a method for detecting brain tumors using MRI that is based on the clustering technique of fuzzy c-mean and was implemented in a system that processes medical pictures. This method detects brain tumors by comparing the images of the patient to a database of normal brain tissue. The photographs of the patient are compared to a database of photos of normal brain tissue, which allows this technology to identify brain tumors. BCET performs an analysis on the picture that is being input and improves the image's quality all around by applying a median filter. After that, a picture is segmented using an FCM clustering approach, and then a canny edge detector is used in conjunction with that method to produce an edge map of the brain tumor [80-81].

3. METHODOLOGY

The objective of the research that is presented in this chapter is to devise a method for the segmentation of MRI scans and an automated system for the testable prediction of outcomes (for instance, the separation of tumors) that is based on the application of previously developed machine learning techniques. This chapter shows the findings of the study that was carried out in order to achieve the aforementioned objective. It will be necessary to devise both a method for object delineation and an algorithm for prediction in order to be successful in achieving these objectives. The investigation that will be offered in this chapter will concentrate, for the most part, on the procedure of coming up with a variety of different approaches. Research is now being carried out on a variety of subjects connected to threshold iterative segmentation of objects in MRI images, along with other topics of a similar kind. It is a well-known fact that choosing a suitable global threshold for the aim of achieving an optimum design and development process is a very challenging task. This is because there are different degrees of gray both inside the region of abnormality in the imaging data (for example, brain tumors) and in the surrounding area that is not affected. This is as a result of the fact that it is common knowledge that choosing an adequate global criteria is a process that is fraught with difficulty. The explanation behind this is as follows: This is because there is a strong link between the neighboring sections of the pictures that follow after them. This is the reason why this seems to be the case.

It is beneficial for clinicians at any stage of the diagnostic process to be able to distinguish and categorize the edges of items of interest on MRI medical imaging. These edges may be found on images of the human body. A magnetic resonance imaging (MRI) scanner is one such source from which to get these pictures. Examples of such objects include the brain itself as well as a section of the brain that has been infected. It is feasible, with the assistance of segmentation, to identify the area (outline) of these zones with an accuracy that is relatively high.

3.1 PROPOSED METHODOLOGY

The quality of the photos that were taken using medical equipment is going to be the deciding factor in the processing outcome. Because of the technical characteristics of the devices, the final photos (or groups of images) almost always include discernible noise. This is the case in the majority of situations, as shown in Figure 3.1. This was done in order to improve the diagnostic analysis accuracy on MRI images.

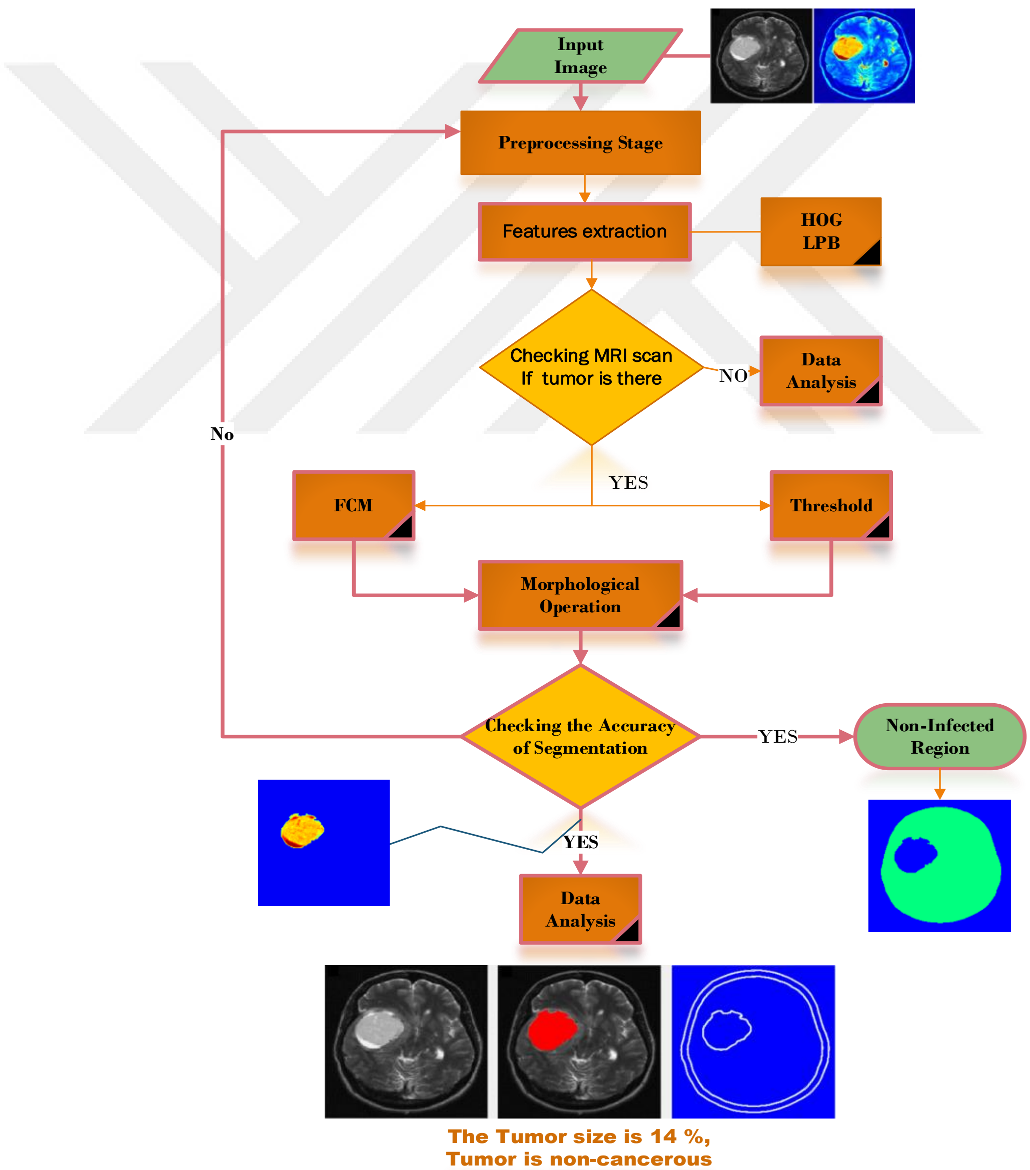

Figure 3.1: The diagram of the brain tumour segmentation and analysis on MRI images.

There are a variety of approaches that may be used across a variety of diagnostic systems for the identification or segmentation of brain tumors. Our proposed algorithmic strategy segments things, such brain tumors, with a high degree of precision and takes their features into consideration. In order to enhance the diagnostic analysis accuracy on MRI images, we reported the use of the following technique for analyzing local entities (tumors) on MRI images, which may help to reduce the effects of noise on the analysis findings. Because of how the segmentation process works, this is really doable. When people talk about "outlining," they are referring to this general idea. It has been demonstrated that the results obtained are reliable and sufficient, despite the fact that there is a large variety of processes, which have been narrowed down to only include those that provide the most favorable results. Despite this, it has been shown that the results obtained are sufficient. Only those methods that provide the best possible outcomes have been taken into consideration, despite the fact that there is a large number of options to choose from.

Most of the time, a picture of the tumor and a report detailing the doctor's assessment of the image is given to the patient when doctors are trying to make a diagnosis. The suggested technique will aid the doctor in detecting patients with cancer and will allow the doctor to train the system using a minimal amount of patient data. After running the data through the system's paces, a report on the clinical condition is generated and shared with the treating medical staff.

The section of the image depicting the tumor is often far more striking than the rest of the image. The foundational components of the cancer detection algorithm are applied here. These stages have been written into the code that makes up the program, as well as the algorithm that was developed. During this interim period, further processing could be performed on the section of the item of interest that is of interest because it includes the component that is anticipated to be present. The metrics that are necessary for the analysis are taken into account when the processing is being done.

3.2 IMAGE CONTRAST ENHANCEMENT

The primary objective of preprocessing is to enhance the picture quality of the local region being investigated (in this case, tumors of brain malignancies) using MRI technology. In addition, a form that can be further processed by machine vision systems or by people is produced. In addition, several MRI characteristics may be enhanced by the use of preprocessing [82]:

After that, in order to improve the signal-to-noise ratio, we use an adaptive contrast enhancement technique that is based on the modified function (described in [83]). Therefore, bringing about an improvement in the clarity of the first MRI scans. However, the most significant barrier is the low picture quality, which makes it difficult to extract, analyze, and identify characteristics in an effective manner, and to quantitatively quantify them. Medical pictures are often corrupted by impulsive, multiplicative, or additive noise as a result of the flawed imaging process features that cause them to be created. The authors of the paper [37] suggested using a method known as the Contrast Balance Enhancement Technique (CBET) in order to achieve a higher contrast level while emphasizing the region of interest. It is important to point out that the region of interest calls for contrast while doing medical imaging.

The Contrast Limited Adaptive Histogram Equalization (CLAHE) approach was discussed in the works [84, 85]. The purpose of the procedure was to enhance the features and identify superior medical imaging qualities, which would ultimately result in an accurate diagnosis. Unsharp masking is an additional fascinating technique that may be used for the purpose of picture improvement. The use of a high-frequency emitter makes this approach particularly susceptible to noise, despite the fact that the purpose is to increase the detail and edges of the image. The author demonstrated in his study [86] that invariant contour transform, also known as STICT, improves the overall quality of MRI images.

We make use of the algorithm in the procedure that was recommended (BCET). It is possible to reduce or increase the contrast of a picture without affecting the appearance of the histogram of the original input image (I old). The problem is solved by deriving a parabolic function from the input picture in this approach. The equation for the parabolic function may be put down as follows:

$$I_{New} = a \cdot (I_{old} - b)^2 + c \ . \tag{3.1}$$

The coefficients a is derived from the input. Whereas b and c are determined from the minimum output image value (I_{New}), the maximum output image value. The following equation calculates the value of the average output image:

$$b = \frac{h^2 \cdot (E-L) - s \cdot (H-L) + l^2 \cdot (H-E)}{2 \cdot \left[h \cdot (E-L) - e \cdot (H-L) + l \cdot (H-E)\right]}, \tag{3.2}$$

$$a = \frac{H-L}{(h-l)(h+l-2b)}, \tag{3.3}$$

$$c = L - a(l-b)^2, \tag{3.4}$$

$$s = \frac{1}{N}\sum_{i=1}^{N} I_{Old}^2(i). \tag{3.5}$$

where h and l are the maximum and minimum of the input image, respectively. Additionally, H and L are the maximum and minimum values of the output image. While s refers to the average of the input image, e denotes the mean square sum of the input image.

3.3 FEATURE EXTRACTION

The preprocessed Computed tomography data in this investigation yields both local and global properties. HOG and LBP feature extraction methods are described in-depth in the following subsections.

3.3.1 HOG Features

Object recognition algorithms make use of the Histogram of Oriented Gradients in order to classify the patterns that are seen in photographs (HOG). A medical picture is evaluated to determine the frequency with which the orientation of each gradient occurs in a certain region. The HOG feature extraction module provides a solution that is both fast and straightforward for the process of extracting features. Because of the core calculations, it is a more quicker and more effective feature descriptor than SIFT and LBP [87]. HOG characteristics have also been shown to be beneficial as detection descriptors in a number of studies. The two applications that make the most frequent use of this technology are image processing and computer vision. HOG is a term that may be used to describe the form and look of the picture. The picture is then broken up into many smaller cells, such as the 4-by-4 grid that was used for this study, and the edge directions are determined in this manner. Histograms may be normalized, which is one way to improve the accuracy of the data they provide.

The local object appearances and forms may be characterized by using the histogram of directional gradients' descriptor, which is based on the dispersion of intensity changes or data. In order to construct a gradient direction histogram for each cell, the image must first be cut up into tiny connected chunks that are referred to as cells. In the next step, we classify the fashion items in the F-MNIST dataset using SVM, basing our decisions on the numerous characteristics of the retrieved photographs. It is required to do some preprocessing work before to collecting picture samples in order to eliminate noise artifacts prior to training a classifier and assessing the test. This is because collecting image samples is the first step in the process. When pre-processing is applied, the resulting feature vectors for training classifiers are significantly improved. It is vital to do sufficient preprocessing if one want to enhance identification rates and cut down on the number of incorrect classifications. In the suggested research, identifying fashion goods is accomplished via the use of HOG-based feature extraction. When attempting to extract the HOG feature from an image, images with a resolution of 2828 pixels are employed [88], [89].

Integrating all of this information results in the construction of the descriptor. By first giving an estimate of the intensity over a larger region of the image, which is referred to as a block, and then utilizing this value to normalize each cell inside the block, local histograms have the potential to make a major increase in the accuracy of the analysis. The inversion of the changes in light and shadows is improved as a result of this normalization. Figure 3.2 depicts the process that must be gone through in order to get HOG characteristics.

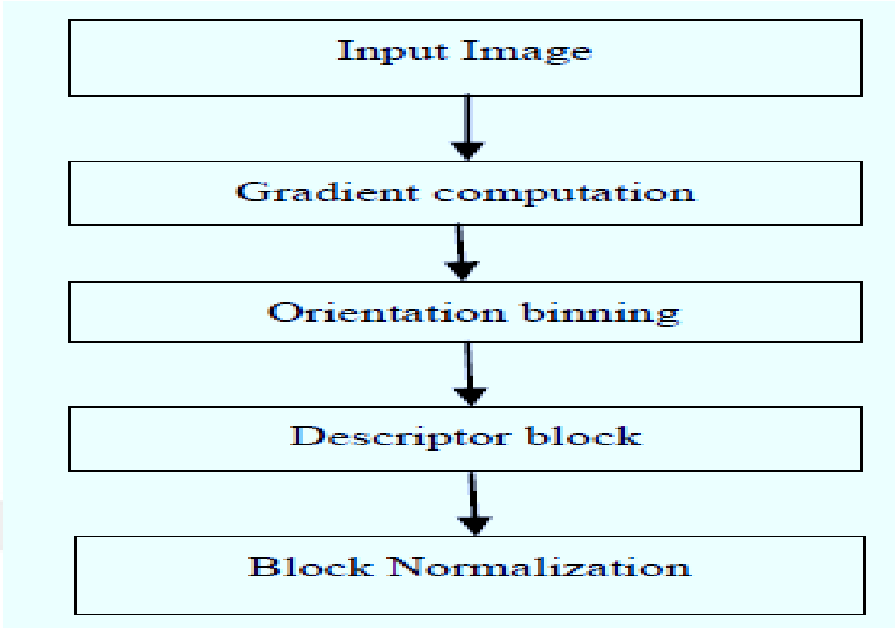

Figure 3.2: HOG feature extraction.

Gradient Computation : The visual window was divided into several little spatial sections that are referred to as cells. Within each cell is a one-dimensional distribution of a gradient or border orientation over its individual pixels. Keeping track of the grade values is done throughout the whole of the calculation procedure. The employment of a one-dimensional centered, pointed discontinuous derivatives mask in both the horizontal and the vertical axes is by far the most prevalent approach. We used background subtraction to generate the gradients, and after that, we put them through a series of tests using a wide range of discrete masking derivatives. In order to ensure the efficiency of the kernels in this technique, the data pertaining to color or intensity must be filtered:

Orientation Binning : The following phase in feature extraction in statistical analysis is called cell calculation, and it's an important element of the process. The values of the edge direction histogram channel are compiled into orientation bins over minuscule spatial areas that are referred to as cells depending on the direction of the gradation element that is centered on each cell. There is a possibility that they will take on a radial or rectangular form. Depending on whether the gradients are "unsigned" or "signed," the rotation bins may range from 0 to 180 degrees or from 0 to 360 degrees and have an equal spacing between each bin. For the range ranging from 0 degrees to 180 degrees, the picture pixel size squares are 128 by 128 and there are nine direction bins. The orientation bin that should be assigned to each pixel is determined by using the pixel's alignment as a starting point.

Descriptor Block: In order to modify the gradient strengths of the HOG features, it is required to merge cells into bigger blocks that are spatially related to one another. The HOG specification is constructed using the concatenation of vectors derived from modified cell scatter plots for each area. These blocks tend to overlap one another, which is indicative of the fact that each cell is discussed more than once in the overall description. There are several instances of block geometric shapes, such as the rectangular R-HOG blocks and the circular C-HOG blocks. In this investigation, the ideal configurations for 2x2 holding cells of 4x4 pixel cells using 9 percentile channels are determined via the utilization of the rectangular R-HOG. There are a total of 36 HOG feature sets produced from each CT scan image.

Block Normalization: There are four main methods for doing block equalization. A small constant (e) is placed in front of V, which represents all the histograms in a given block, and the non-normalized vector V is used to represent all the histograms in this block (the exact value, hopefully, is unimportant). After that, you may choose an adjustment factor from the following list:

$$L2 - normal: \;\; f = \frac{v}{\sqrt{||v||2+e^2}} \tag{3.6}$$

L2-hys: L2-normal followed by clipping (limiting the maximum values of v to 0.2) and renormalizing, as in

$$L2 - normal: \;\; f = \frac{v}{||v||1+e} \tag{3.7}$$

$$L2 - hys: \;\; f = \sqrt{\frac{v}{||v||1+e}} \tag{3.8}$$

The L2-his approach may be computed by first taking the L2-normal, then compressing the result, and then renormalizing the value. On the other hand, a large range of gradient magnitudes is produced as a result of the significant differences in the depth of field. The histograms of each cell are normalized such that the issue may be solved by merging the histograms of cells that are next to one another into a larger block. In the last step, the chosen CT slices are joined together to produce the HOG-based bounding boxes.

3.3.2 LBP Features

As its name indicates, a Local Binary Pattern (LBP) is a method that may be used to describe the appearance of an image inside a condensed area that surrounds each particular pixel. The primary principle upon which basic banalization is built is the idea that textures represent two distinct local things—namely, a pattern and the strength of a pattern—and this idea is what underpins basic banalization. The production of local binary patterns is accomplished by using an imaging block that is composed of three pixels and is controlled by the operator. The value of the center pixel is thresholded, then it is multiplied by powers of two, and lastly it is concatenated in order to generate a label for this pixel. This process is repeated in order to produce a label for this pixel. There is a total of 256 possible labels that can be produced by using the respective gray values of the center and the pixels in the neighborhood [88], [89]. This is due to the fact that the neighborhood is composed of 8 pixels. In addition to this, the procedure of classification takes into consideration the mean as well as the standard deviation of the LBP-Local characteristics that are present in an image. At the pixel level, LBPs are the ones to thank for the translation of a grayscale image into a matrix of numerical integers. In the form of a label matrix, you may get a description of the original photo that you're looking for here. It does this by figuring out how to represent the texture in some form or another on a map. It is common practice to incorporate some type of graphic description in curriculum vitae as a way to organize the information that is given. When the HOG feature descriptors are used, there is a discernible and substantial increase in the level of performance.

LBP is a feature descriptor that is used to classify textures and has a strong defining characteristic. When interpreting CT scans, it is essential to take into consideration the patient's tissue's texture. It has been discovered that LBP is an effective extension for classification issues because to the fact that it is invariant to both grayscale and rotation [90]. According to the results of the LBP sampling stations, the textural qualities are determined by the radius N that surrounds the center pixel (neighborhood pixels) $LBP_{N,R}$:

$$LBP_{N,R}(x_c, y_c) = \sum_{k=0}^{N-1} s\big(x(k) - x(c)\big)2^k \quad , \qquad s(x) = \begin{cases} 1, x \geq 0 \\ 0, x \prec 0' \end{cases} \tag{3.9}$$

where R is the diameter of the circle and N is the total number of points sampled within that diameter range. R is the variable that affects the quantization of angular space, and it is R that controls the pixel density of LBP. As a direct result of this, the accuracy of categorization is significantly impacted by the aforementioned two parameters. The values of pixel K and pixel C, respectively, are denoted by the notations X (K) and x(C), respectively. The invariants of LBP with regard to grayscale and rotation are guaranteed to be invariant by the function s. (x). In this particular scenario, the value of s(x) is considered to be 1 if it is greater than or equal to the value of the pixel x. (K). In all other cases, the value of s(x) is 0.

3.4 SUPPORT VECTOR MACHINE (SVM)

On the basis of extracted characteristics, the support vector machine (SVM) classifier has been employed for tumor predication on medical images (LBP and HOG). The support vector machine (SVM) is a kind of non-probabilistic binary linear classifier. To train an SVM, a collection of examples is split into two categories, and then a model is developed that places new cases into one of the categories. Support vector machines may be used to produce hyperplanes and hyperplane sets for classification applications that take place in a space with a high or an infinite number of dimensions. SVMs are an effective supervised learning approach that may be used in conjunction with machine learning to discover patterns hidden inside data. The hyperbolic plane is attainable in the event that enough separation is maintained together with the largest possible distance from neighboring training data in any category.

A higher margin of error will help reduce the number of incorrect generalizations. Figure 3.3 illustrates the maximum boundary classifier that may be used. Classifiers such as the support vector machine (SVM), which may be used for both classification and regression, are often used in supervised learning [91]. Utilizing the Supporting Vector Machine may be beneficial for a variety of different kinds of recognition, such as word recognition, recognizing faces, and so on. It produces outstanding outcomes when applied to situations that are based on the actual world [92]. In this section of the course, we will train and test using a support vector machine. This strategy included classifying the fashion pictures contained inside the F-MNIST database into HOG feature space by using a multiclass SVM classifier. To fill up the whole feature space, HOG features with dimensions of 1296 by 1296 have been laid up in rows. Figure 3.3 presents a schematic of the SVM classifier for your viewing pleasure.

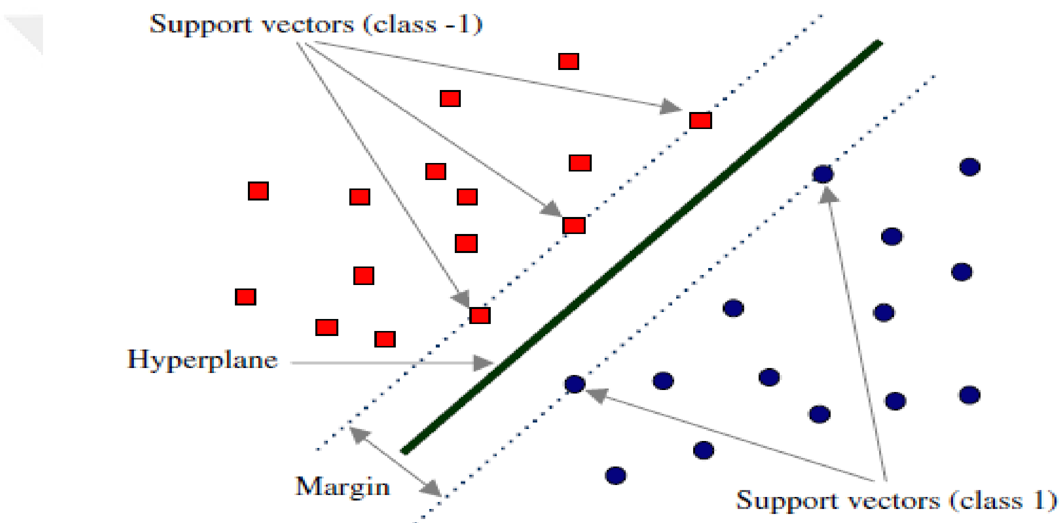

Figure 3.3: Maximal Margin Classifier (SVM).

3.4.1 Multi - Class SVM

Instead of creating many binary classifiers, it makes more sense to do a single optimization technique to separate all of the categories [93]. All k-binary SVMs may be learned at the same time using these techniques, which offer a clear goal variable and maximize offsets from each category to the remaining items for a k-class problem. Assuming a labeled training set, $\{(x_1, y_1), \ldots. (x_n, y_n)\}$ of cardinality l, where $x\_i \in R\^d \; and \; y\_i \in \{1, \ldots, k\}$, the formulation proposed in [94] is given as follows:

$$\min \frac{1}{2} \sum_{m=1}^{k} W_m^T W_m + C \sum_{i=1}^{1} \sum_{t \neq y_i}, \qquad (3.11)$$

$$W_m \in H, b \in R^k, \aleph \in R^{lxk}$$

$$\text{subject to} \quad W_{y_i}^T \varphi(x_i) + b_{y_i} \geq W_t^T \varphi(x_i) + b_t + 2 - \aleph_{i,t} \tag{3.12}$$

$$i = 1, \ldots, l, t \in \{1, \ldots, k\} \setminus y_i.$$

The result of the decision is:

$$\arg\_max_m f_m(x) = \arg_{max\ m}\left(W_M^T \varphi(x) + b_m\right) \tag{3.13}$$

3.5 BRAIN TUMOR SEGMENTATION METHOD

CT scan segmentation is a technique that is regularly used to identify the limits of an image as well as the components that are included inside it (curves, lines, etc.). The separation of medical pictures in order to distinguish a local item (brain tumors utilizing MRI images or other clinical imaging technologies) is an essential step [95, 96]. This is because selecting the appropriate treatment choice should be simple.

Picture delineation, which refers to the act of identifying a region of interest in a medical image either manually or by computer means, is crucial (ROI). Isolating certain anatomical features has been accomplished via the use of a number of different picture fragmentation techniques, which have been described in medical journals. This technology has a wide range of applications, some of which include fully automated blood cell categorization, mammography mass detection, camera calibration, cardiac segmentation and analysis, coronary computed tomography feature extraction, patient management, surgery information processing, target organ damage and data processing, brain and animal improvement experiments, properly functioning mapping, and a great deal more [97, 98].

The authors of the thesis created a threshold iteration approach that differentiates between sick and uninfected regions of MRI and CT data by using better forms of Otsu and C-means fuzzy clustering. The method may be found in the thesis.

Allow L grayscale values $[1, 2, \ldots, L]$ to represent the image's tonal range. The fraction of dots that are a shade of gray (xi) (i). The sum of all possible points is denoted by the formula $X =$

$x\ 1 + x\ 2 + +x\ L$. The histogram of the grayscale picture is used to model the distribution of events:

$$q(i) = \frac{x_i}{X}\ , x_i\ \geq 0, \sum_{i=1}^{L} x_i = 1. \tag{3.14}$$

Using a threshold value of t, image pixels are split into the foreground and background components, respectively denoted by C 0 and C 1. Pixels inside levels [1,2,....., t] are re-presented in C 0, whereas those within levels [t + 1,... L] are shown in C 1. The following equations determine the class and intermediate occurrence probability, accordingly.

$$m_0 = m(t) = \sum_{i=1}^{t} q(i), \tag{3.15}$$

$$m_1 = 1 - m(t) = \sum_{i=t+1}^{L} q(i), \tag{3.16}$$

$$\mu_0 = \sum_{i=1}^{t} \frac{i.q(i)}{m_0} = \frac{1}{m(t)}\ , \tag{3.17}$$

$$\mu_1 = \sum_{i=t+1}^{L} \frac{i.q(i)}{m_1} = \frac{1}{1-m(t)} \sum_{i=t+1}^{L} i.m(i)\,. \tag{3.18}$$

The overall average is defined:

$$\mu_T = \sum_{i=1}^{L} i.m(i). \tag{3.19}$$

and then me can find:

$$\mu_T = m_0\mu_0 + m_1\mu_1\ , \tag{3.20}$$

where m 0 and m 1 - represent the probability of being in the front or distance, respectively. Further, _0 and _1 stand for the typical grayscale value of the depth of field, correspondingly. Here, we have a full grayscale picture denoted as μ_T,.

4. RESULTS AND DISCUSSIONS

In this preliminary research, segmentation evaluated a large number of items using binary data (brain tumors). The Digital Imaging Common Open Metadata (DICOM) [99] repository is one example of such a trove. In order to achieve their conclusion, the researchers looked at 150 photographs from the DICOM collection of patients with brain tumors.

The Brain-web dataset [100] is another example of a dataset that has been used in research. It is composed of sequentially modeled data from three separate modeling modalities, all of which are comprehensive 3D MRI scans of the brain. Examples of such sequences are T1-weighted MRI and T2-weighted MRI. Of the 48 photos up top, 15 are really close-ups of brain tumors. The second group of brain tumor statistics was compiled by radiologists and had 10 case studies, each of which included 6 images. The first 75 images were taken from MRIs and a digital database of screening mammography (DDSM) [101, 102]. These images were used to make a magnetic resonance imaging (MRI) scan of the brain. Due to the fact that the MRI scan is not a precise tomogram and instead contains varying contrast and, in this example, segmentation, the results of employing different implementations of BCET are illustrated in Figures 4.1. That's because it's always preferable to move to a new implementation rather than merely tinker with the thresholds that are already in place.

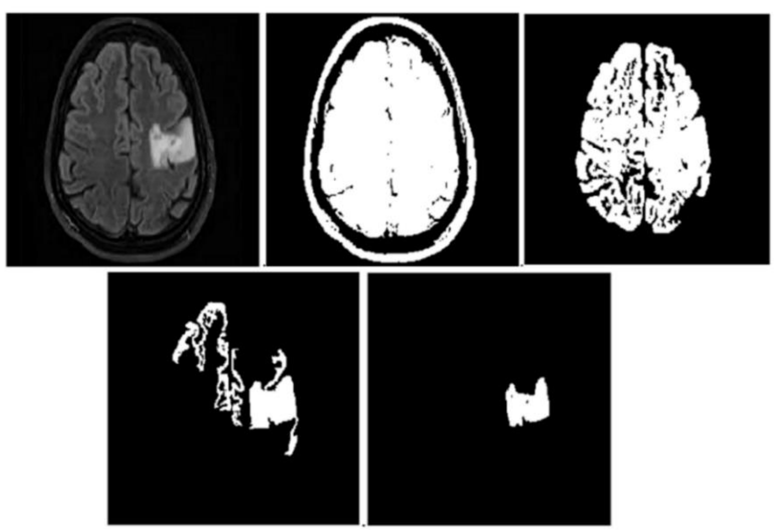

Figure 4.1: An example of segmentation of an object (brain tumor) using different value of mean.

In this preliminary research, segmentation evaluated a large number of items using binary data (brain tumors). The Digital Imaging Common Open Metadata (DICOM) [99] repository is one example of such a trove. In order to achieve their conclusion, the researchers looked at 150 photographs from the DICOM collection of patients with brain tumors.

The Brain-web dataset [100] is another example of a dataset that has been used in research. It is composed of sequentially modeled data from three separate modeling modalities, all of which are comprehensive 3D MRI scans of the brain. Examples of such sequences are T1-weighted MRI and T2-weighted MRI. Of the 48 photos up top, 15 are really close-ups of brain tumors. The second group of brain tumor statistics was compiled by radiologists and had 10 case studies, each of which included 6 images. The first 75 images were taken from MRIs and a digital database of screening mammography (DDSM) [101, 102]. These images were used to make a magnetic resonance imaging (MRI) scan of the brain. Due to the fact that the MRI scan is not a precise tomogram and instead contains varying contrast and, in this example, segmentation, the results of employing different implementations of BCET are illustrated in Figure 4.2. That's because it's always preferable to move to a new implementation rather than merely tinker with the thresholds that are already in place.

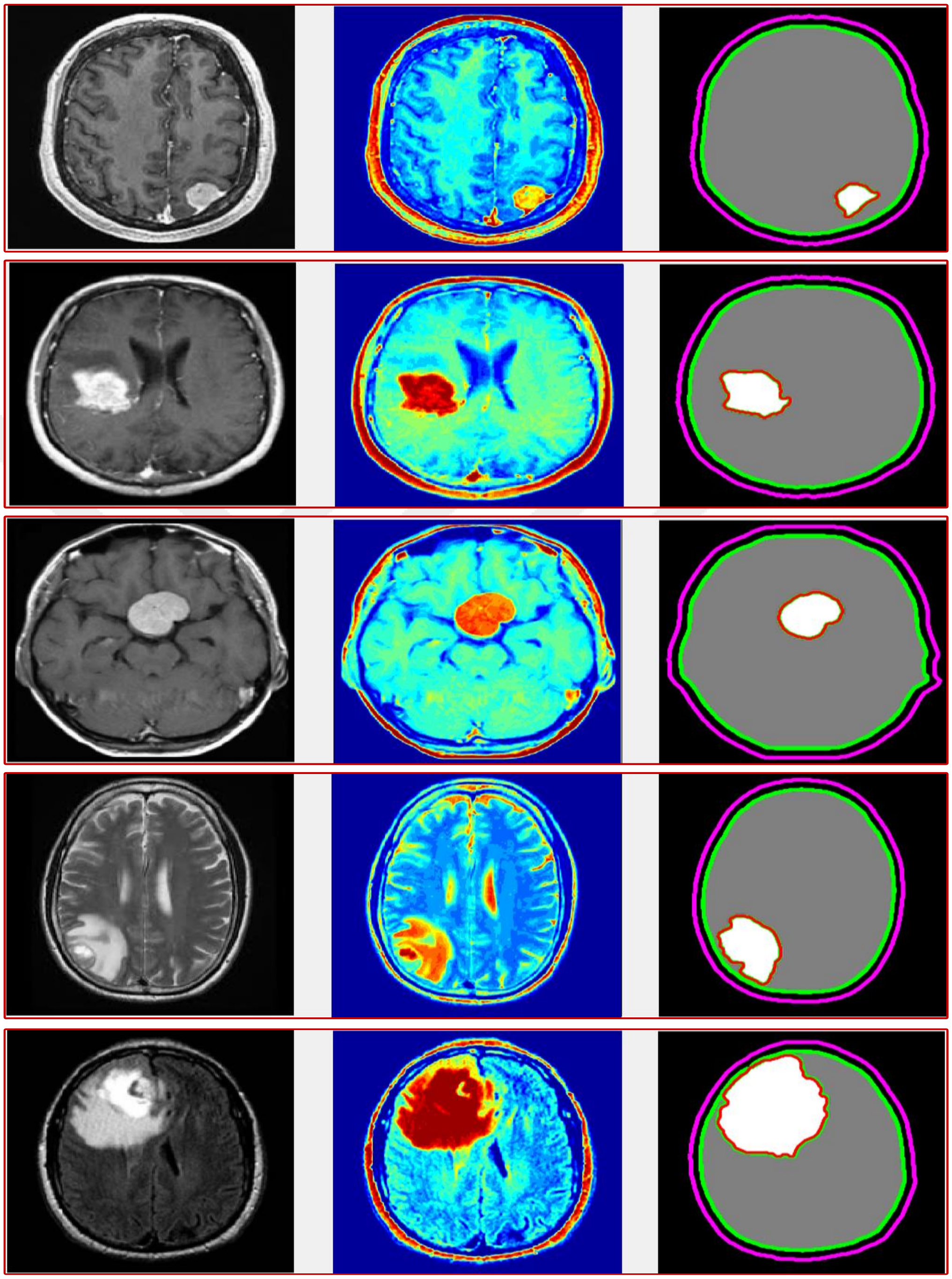

Figure 4.2: The red line indicates the diseased region, while the green line indicates the unaffected region of brain in certain examples where the approach was used to pinpoint the location of the item (a brain tumor).

Figures 4.3 and 4.4 are the example of the developed software program under MATLAB 2021 platform that contain more than one result for tumor analysis, which helps the radiologist and specialist in diagnosing the disease and preparing a plan to treat the patient and keep him away from danger and maintain his health.

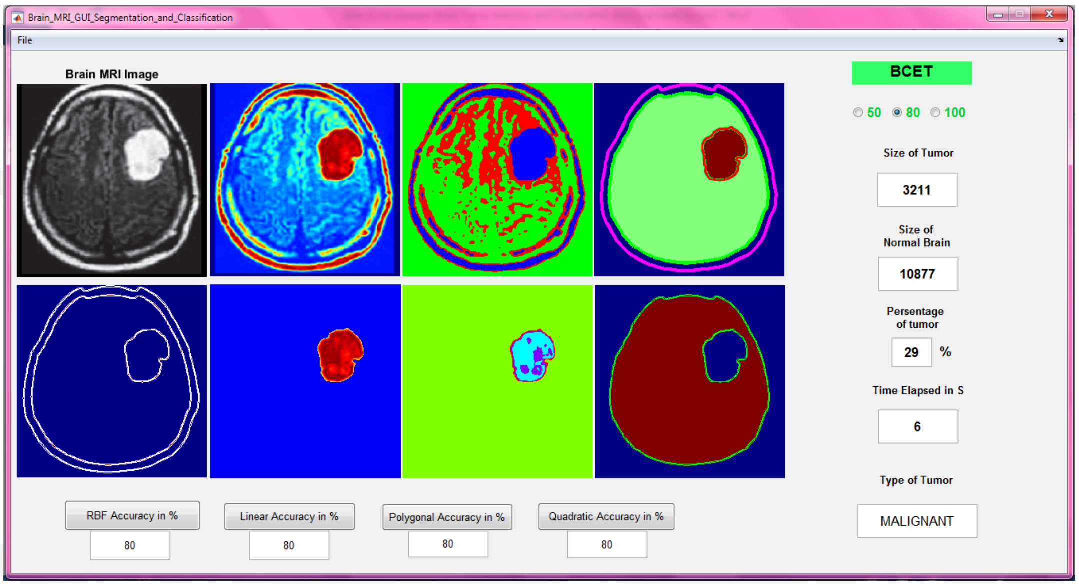

Figure 4.3: Example 1 of developed SM platform for mass analysis.

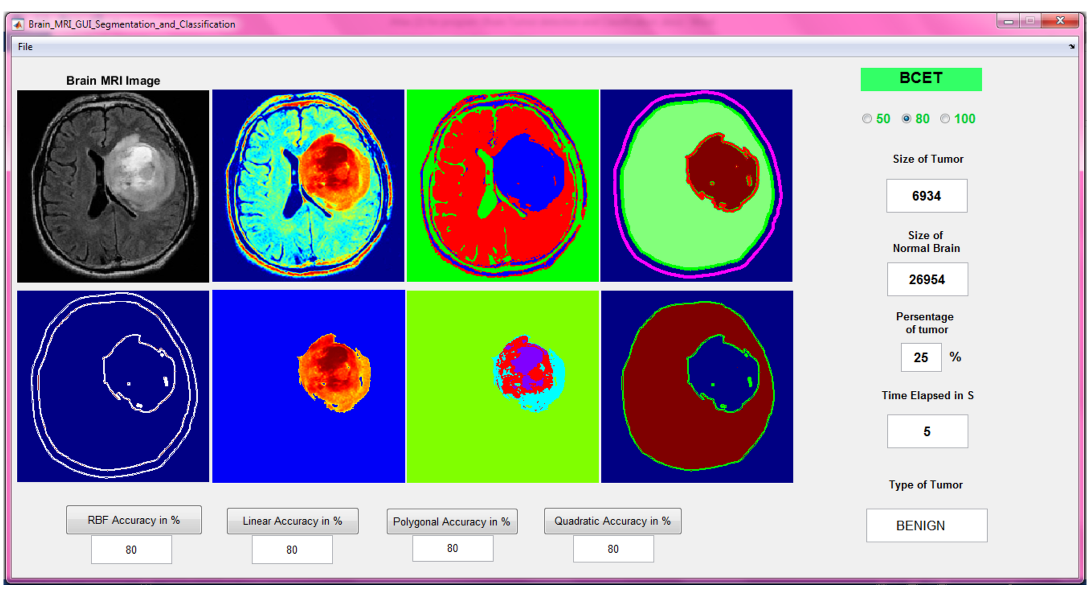

Figure 4.4: Example 2 of developed SM platform for mass analysis.

Our method effectively identifies the tumor region (in in addition to the healthy brain inside the original input image) with a color consequence that is presented in Figures 4.3, in contrast to the current state of the art methods, which leave some non-neoplastic region on the segmented image that is perplexing for diagnosis (there are no tumor boundaries and normal regions of the brain). The observations make it quite clear that in terms of its ability to discern between normal and abnormal areas, our algorithm is much better to other methods that have been tried in the past (tumors).

In order to determine the validity and accuracy of the tumor, along with the map of the normal area of the brain and the edge of the tumorigenesis mas that were created by our method, the following factors were used in the evaluation process:

The structured similarity index comes in first (SSIM).

i. Mean square error (MSE).

ii. Peak signal-to-noise ratio (PSNR) in dB.

iii. The ratio of pixels that were detected (PCD).

iv. The ratio of pixels that were not detected (PND).

v. Probability of False Positive Results (PFA), and Merit Score (MS).

vi. The combination of sensitivity and accuracy.

These seven measures are mostly determined by the values of TP, TN, FP, and FN:

True positive (TP) refers to the number of pixels that accurately recognized the tumor boundary; negative (TN) indicates the number of pixels that accurately detected the background;

False positive (FP): As its name suggests, this refers to the number of pixels that are incorrectly recognized as the boundary of the tumor. False negative (FN): This refers to the number of pixels that are incorrectly identified as the background.

The Structural Similarity Index, often known as SSIM, is a perceptual metric that measures the degree to which picture quality degrades as a result of data transmission loss, compression loss, or any other image processing approach. The SSIM is defined by the following equation:

$$SSIM(x,y) = \frac{(2\mu_x\mu_y + C_1)(2\sigma_{xy} + C_2)}{(\mu_x^2 + \mu_y^2 + C_1)(\sigma_x^2 + \sigma_y^2 + C_2)}. \tag{4.1}$$

When the SSIM score is greater, it indicates that the brightness, structural content, and contrast have been retained more successfully.

In most cases, the Root Mean Square Error will be used to determine how accurate a picture or signal is (MSE). Offering a mathematical estimate is one way to assess accuracy in an image or signal, which serves the goal of determining the degree of similarity between two pictures and is done for the purpose of evaluating the correctness of an image or signal. One of the photos is supposed to be the original for the purpose of computing the MSE, whereas the other image has been rotated, cropped, or otherwise altered in some way. The MSE is defined as follows:

$$MSE = \frac{1}{N}\sum_{i=1}^{N} E_i^2 = \frac{\|E\|^2}{N} \ . \tag{4.2}$$

Peak Signal-to-Noise Ratio (PSNR) is used to evaluate image reconstruction quality. It is calculated as follows:

$$PSNR = 10\log_{10}\left(\frac{(2^n - 1)^2}{MSE}\right) = 20\log_{10}\left(2^n - 1\right) - 20\log_{10}\left(\frac{\|E\|}{\sqrt{N}}\right). \tag{4.3}$$

Higher PSNR and Smaller MSE refer to better signal to noise ratio.

where RE_{Cnt} и AE_{Cnt} – number of ideals (standard) and real point on the edge;

The range of the measurement is from 0 to 1, and the greatest value is considered to be ideal. The sensitivity may be represented by the following equation, which also serves as its definition:

$$Sensitivity = \frac{TP}{TP+FN}. \tag{4.4}$$

The accuracy is shown as a fraction of the total number of outcomes. whereas the fraction of pixels in the foreground and background that are properly recognized is referred to as Precision. The value of the measurement might go anywhere from 0 to 1. When the accuracy value is set to 1, the signal at the output becomes identical to the signal at the input. As a result, the following constitutes the accuracy:

$$\text{Accuracy} = \frac{TP+TN}{TP+TN+FP+FN}. \tag{4.5}$$

The observed results make it abundantly evident that diagnosing the normal region and tumor of the brain using MRI of the brain is accurate and quick in comparison to manual detection conducted by clinical professionals. This conclusion can be drawn from the findings.

The Intersection-over-Union (IoU), also recognized as the Jaccard index or Jaccard similarity correlation, and the Dice similarity coefficient (DSC), also recognized as the F1 score or the Srensen-Dice index, are two most popular metrics that are used in Improperly and are based on the F-measure. Both of these metrics are utilized in the field. The IoU penalizes under- and over-segmentation more than the DSC does, which is one of the key differences between the two measures. The DSC is defined as the harmonic mean between sensitivity and accuracy. Despite this, both scores are valid measures, however the DSC is the metric that is used for management information systems assessment in the vast majority of scientific articles.

$$IoU = \frac{TP}{TP+FP+FN} \ . \tag{4.6}$$

$$DSC = \frac{2TP}{2TP+FP+FN} \ . \tag{4.7}$$

The evaluated performance aspects also indicate that the PSNR, MSE, and SSIM parameters are improved as a result of using it. The method that was proposed provides accurate and speedy object identification (tumors in the brain), and it pinpoints the precise position of both normal regions and tumors in MRI images.

The study of acquired pictures' efficiency at the edges is outlined in Tables 4.1. This analysis involves estimating the tumor area and the area without pathology (brain).

Table 4.1: Parameters evaluation for analysing identified tissues, excised tumours, and pathology-free regions shown in Figure 4.3.

Images	Size of Tumor %	#PSNR	#MSE	#SSIM	#DSC	Execution time (s)
Img 1	5 %	68.990	0.920	0.9765	0.9762	2
Img 2	7 %	65.004	0.35	0.9775	0.9839	3
Img 3	8 %	66.066	0.215	0.9800	0.9898	2
Img 4	18 %	67.03	1.172	0.9863	0.9850	3
Img 5	36 %	68.256	0.245	0.9896	0.9758	3

It is feasible to build a map of the boundaries of the object of interest (malignant region and normal regions) with a correctness that is on average 3-7% greater with the assistance of the approach that was recommended. In addition, the strategy that has been suggested demonstrates a reduction in the amount of brain pixels that are erroneously classified as being part of the sick area of the brain. The improvement is less than one percentage at noise levels that are lower than ten percent. The sensitivity index, on the other hand, demonstrates a decline that is more noticeable yet still remains within the acceptable margin of error.

Table 4.2 presents an overview of recent approaches that have been developed since 2016 for solving a variety of medical picture segmentation challenges by using a convolutional neural network in conjunction with other segmentation algorithms.

Table 4.2: Segmentation of clinical images is a modern technique that makes use of a wide variety of techniques.

Year	Methods	Modality	Accuracy (%)	Metric Evaluation
2017 [14]	Genetic-Algorithm	MRI	91.03	DSC
2018 [38]	2 conductive-U-Nets	MRI-T1-T2	93.32	DSC
2019 [47]	FCMT	MRI-T1-T2	78.20	IoU
2018 [70]	FCM	CT Scan	92.28	DSC
2020 [100]	V-Net	MRI-T1-T2	84.55	DSC
2019 [75]	FCM	MRI	90.63	DSC
2021 [55]	Enh. FCM	MRI	91.33	DSC
2016 [60]	B-CNN	MRI-T1	94.89	DCS
The Presented methodology	FcMT	MRI and CT scans	97.56	DSC
			96.85	IoU

Table 4.2 demonstrates that the created approach has a very high level of accuracy, with an error rate of just 3-4% when segmenting medical pictures.

The training was carried out using a combined set of MRI images taken from the digital imaging in medicine (DICOM) dataset. The purpose of this was to assess how accurate the SVM classifiers were in determining whether or not an MRI scan included a tumor.

Table 4.3 displays, with accompanying explanations, the findings and information pertaining to the categorization of brain tumors.

Table 4.3: Evaluation of SVM classifier for tumour identifying on CT images.

Images	Quantity images		with combined feature (LBP+HOG)		Classification accuracy
	Train	Test	correct	Not correct	
With Tumor	180	80	78	2	0.9750
Without Tumor	452	83	77	6	0.9277
Total amount	632	163	155	8	0.9516

According to Table 4.4, the tumor testable prediction accuracy is 98% on photos with mass and 93% on images without tumor. This is evident from the fact that 95% classification accuracy was achieved on average in the experimental trials while using integrated feature extraction.

Combined extraction of features may successfully identify whether an MRI scan has malignancies around 3%–4% of the time. In Figures 4.5 and 4.6, we see the HOG feature-based and combination feature-based (HOG + LBP) versions of the tumor prediction Confusion Matrix.

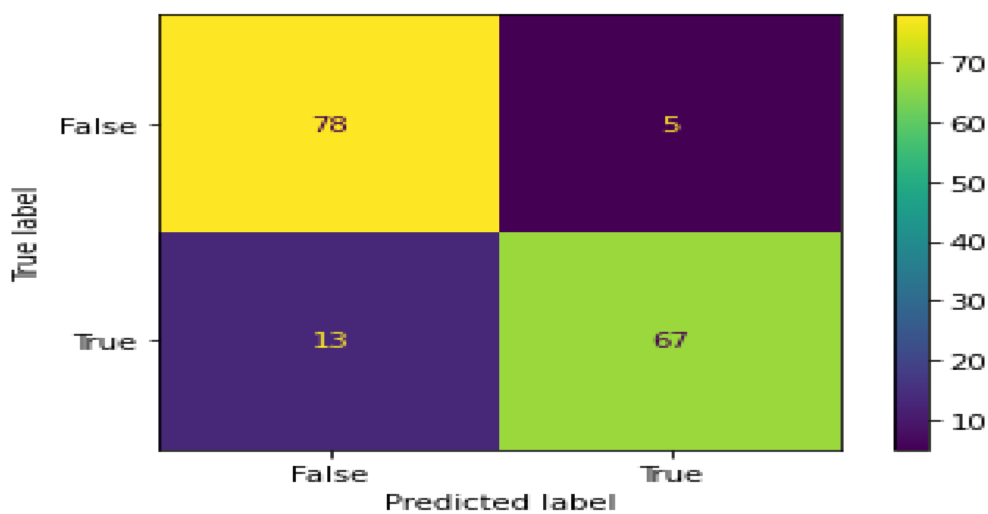

Figure 4.5: Confusion matrix of tumour predication using HOG features.

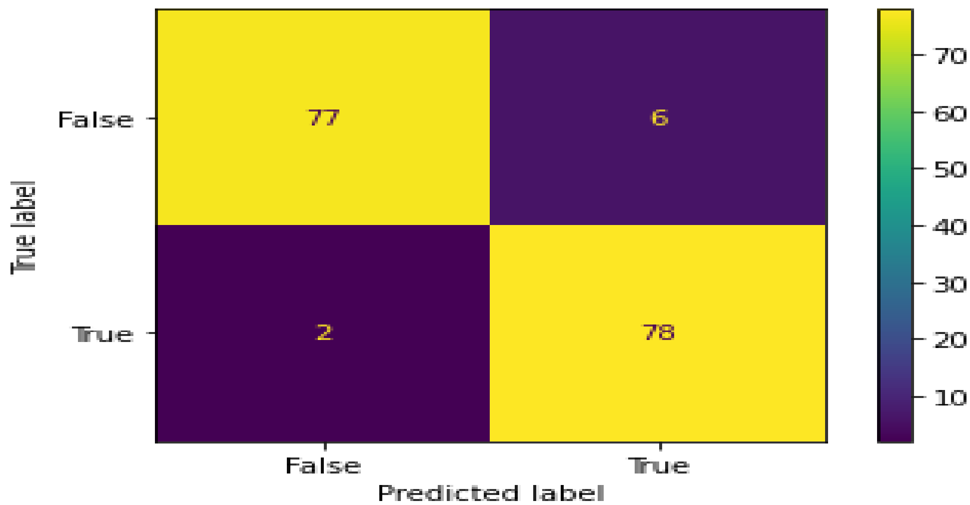

Figure 4.6: Confusion matrix of tumour predication using combined HOG+LBP features.

From Figures 4.5 and 4.6, we can recognize the modified methodology for tumor predication (combination of features HOG and LBP) is more accuracy than using HOG features. The error rate by using combination LBP and HOG is 4 %, while the usual method is 11%.

The evaluation of comparison of our approach with five other models (Multi-Cascaded [103], Cascaded random forests [104], Cross-modality [105], Task Structure [106], One-Pass Multi-Task [107], and Cascade Deep Learning model [108]) using quantitative and qualitative metrics to gain a more in-depth understanding of the tumor segmentation performance. Figures 4.7 and 4.8 show the numerical results of our different proposed structures.

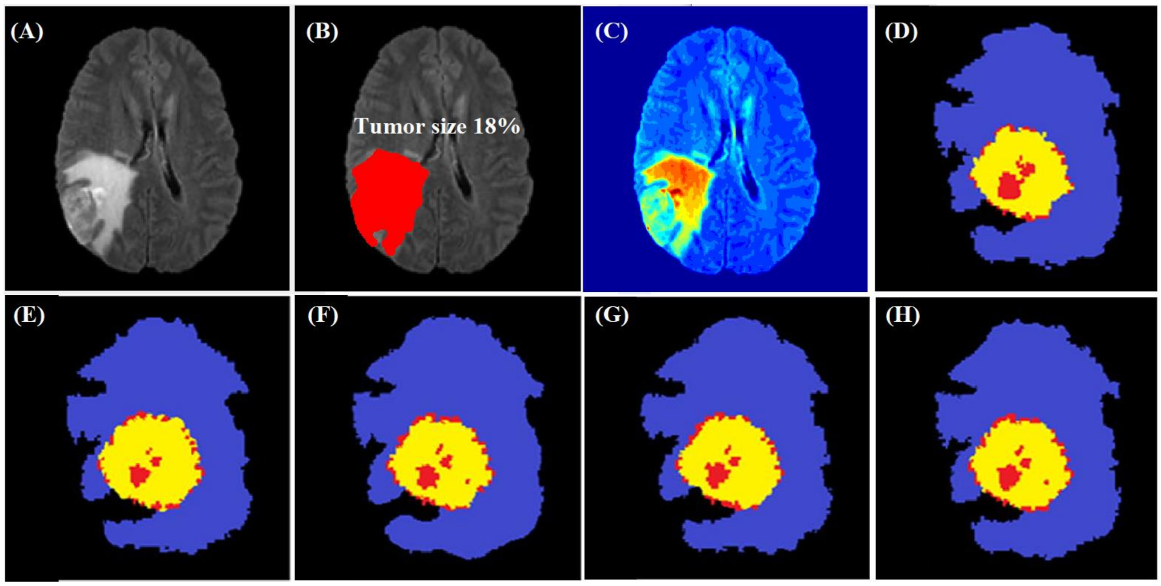

Figure 4.7: Brain tumor localization utilizing the proposed method and four state-of-the-art techniques on BRATS 2018 dataset (the blue, yellow, and red colors are edema, enhanced, and core regions respectively). (A) Input image, (B)&(C) Our method, (D) Multi-Cascaded [103], (E) Cascaded random forests [104], (F) Cross-modality [105], (G) One-Pass Multi-Task [107], and (H) Cascade Deep Learning model [108].

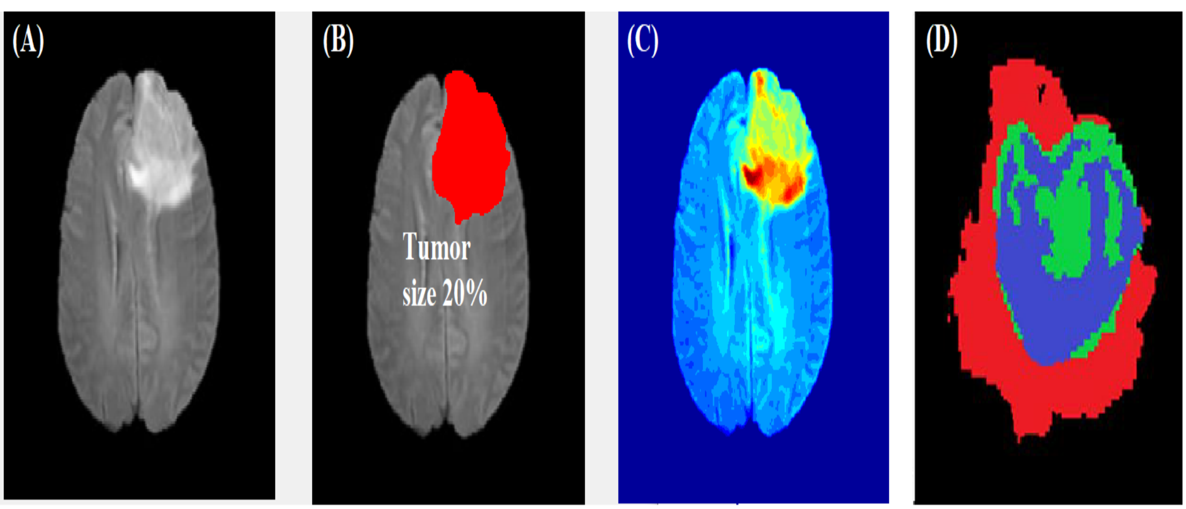

Figure 4.8: The results of segmentation of infected area (brain tumor), using the our method and a Cascade Deep Learning model on BRATS 2018 dataset, (A) Input image, (B)&(C) Our method, and (D) Cascade Deep Learning model

Figures 4.7 and 4.8 graphically displays the successful outcomes of our method on the BRATS 2018 dataset. Each region, as seen here, shares a common boundary with every other region. It is possible to distinguish the demarcation line between the lesion core and the improving areas within the T1C images (third column) with a high degree of accuracy without resorting to the use of other modalities due to the value difference between the two. However, this is not the case when discussing edematous regions, enhanced edematous regions, or the edge of a tumor core. When we take into account the aforementioned features of each modality, me find that a shallower CNN model is sufficient, provided that we restrict our search space sufficiently.

The presented method outperforms previous recently published models, although our algorithm still has certain drawbacks when dealing with tumor volumes larger than one-third of the whole brain. This is because as the tumor becomes larger, the predicted area decreases, resulting in worse extracting features.

5. CONCLUSION AND FUTURE WORK

Clinicians often use subjective criteria for assessing brain tumors. Examining brain scans manually is becoming more time-consuming and frustrating as technology advances. One might counter this by arguing that automated segmentation and classification aid neurologists in their job by facilitating quicker decision making. Recent years have seen significant advancements in the ability to categorize and forecast brain tumors in MRI data because to the application of deep learning algorithms. However, further study is required since MRI is not a simple topic just yet. Medical practitioners may benefit greatly from segmentation and classification methods because they expedite data processing and provide a new viewpoint based on automated outcomes. Malignancies (such as gliomas and meningiomas) are the focus of this thesis, with machine learning for segmentation and classification serving as the primary technique of study. FCMT's groundbreaking work in image processing, especially its emphasis on contrast enhancement, is a powerful asset when it comes to tumor segmentation. The LBP and HOG algorithms are used to extract features for this purpose. All of these individual parts make up the whole that is the ensemble. A convolutional neural network is trained using this Ensemble Features data. There is evidence that a merged SVM using HOG and LBP features may achieve a 97% rate of success in classification. Under 3% of errors are discovered in any one iteration. Max-pooling is a popular process in network topologies; however it usually has the unintended side effect of lowering picture quality and resolution, and hence the network's accuracy. Almost all previous research has only taken into account low-resolution feature maps.

More study is required on this issue. More research is needed to create techniques that preserve an image's quality and allow spatial recognition. Existing CNN-based therapies were frequently designed to treat a specific type of illness. A versatile DL-based framework capable of detecting different tumors would be a huge help to a doctor. Many academic datasets have problems with data imbalance. The Brain Tumor Segmentation (BraTS) dataset is used as a reference, since 96% of the samples are labeled as belonging to a single class and 2% as belonging to another. When creating a model from such an imbalanced dataset, overfitting is unavoidable.

In addition, recent studies have looked at how GANs and other advanced data enrichment technologies can help in the detection of brain tumors. Also, research evaluating the efficacy of various data augmentation strategies in detecting brain cancer is lacking. Moreover, the vast majority of research didn't look into the possibility that various pre-trained state-of-the-art networks may help in diagnosing brain cancer. Data imbalance and limited dataset size are two issues that could be addressed in brain tumor diagnosis with the help of modern data augmentation methods and state-of-the-art pre-trained network architectures.

REFERENCES

[1] K. M. Kurian et al., “Brain tumor research in the United Kingdom: current perspective and future challenges. A strategy document from the NCRI Brain Tumor CSG,” *Neurooncol. Pract.*, vol. 5, no. 1, pp. 10–17, 2018.

[2] Q. Luo, Y. Wang, D. Fan, S. Wang, P. Wang, and J. An, “Prion protein expression is correlated with glioma grades,” *Virol. Sin.*, vol. 35, no. 4, pp. 490–493, 2020.

[3] M. Paolillo, C. Boselli, and S. Schinelli, “Glioblastoma under siege: An overview of current therapeutic strategies,” *Brain Sci.*, vol. 8, no. 1, 2018.

[4] J. Amin, M. Sharif, M. Raza, and M. Yasmin, “Detection of brain tumor based on features fusion and machine learning,” *J. Ambient Intell. Humaniz. Comput.*, 2018.

[5] P. Pedapati and R. V. Tannedi, *Brain Tumour Detection using HOG by SVM*. 2018.

[6] C. S. Rao and K. Karunakara, “A comprehensive review on brain tumor segmentation and classification of MRI images,” *Multimed. Tools Appl.*, vol. 80, no. 12, pp. 17611–17643, 2021.

[7] E. S. Biratu, F. Schwenker, Y. M. Ayano, and T. G. Debelee, “A survey of brain tumor segmentation and classification algorithms,” *J. Imaging*, vol. 7, no. 9, p. 179, 2021.

[8] E.-S. A. El-Dahshan, T. Hosny, and A.-B. M. Salem, “Hybrid intelligent techniques for MRI brain images classification,” *Digit. Signal Process.*, vol. 20, no. 2, pp. 433–441, 2010.

[9] S. Das, M. Chowdhury, and M. K. Kundu, “Brain Mr image classification using multiscale geometric analysis of ripplet,” *Electromagn. Waves (Camb.)*, vol. 137, pp. 1–17, 2013.

[10] A. Zotin, K. Simonov, M. Kurako, Y. Hamad, and S. Kirillova, "Edge detection in MRI brain tumor images based on fuzzy C-means clustering," *Procedia Comput. Sci.*, vol. 126, pp. 1261–1270, 2018.

[11] J. Jiang, Y. Wu, M. Huang, W. Yang, W. Chen, and Q. Feng, "3D brain tumor segmentation in multimodal MR images based on learning population- and patient-specific feature sets," *Comput. Med. Imaging Graph.*, vol. 37, no. 7–8, pp. 512–521, 2013.

[12] A. Ortiz, J. M. Górriz, J. Ramírez, and D. Salas-González, "Improving MRI segmentation with probabilistic GHSOM and multiobjective optimization," *Neurocomputing*, vol. 114, pp. 118–131, 2013.

[13] J. Amin, M. Sharif, M. Yasmin, and S. L. Fernandes, "A distinctive approach in brain tumor detection and classification using MRI," *Pattern Recognit. Lett.*, vol. 139, pp. 118–127, 2020.

[14] M. Chen, Q. Yan, and M. Qin, "A segmentation of brain MRI images utilizing intensity and contextual information by Markov random field," *Comput. Assist. Surg. (Abingdon)*, vol. 22, no. sup1, pp. 200–211, 2017.

[15] P. S. Raja and A. V. Rani, "Brain tumor classification using a hybrid deep autoencoder with Bayesian fuzzy clustering-based segmentation approach," *Biocybern. Biomed. Eng*, vol. 2020, pp. 440–453.

[16] N. Arunkumar *et al.*, "K-Means clustering and neural network for object detecting and identifying abnormality of brain tumor," *Soft Comput.*, vol. 23, no. 19, pp. 9083–9096, 2019.

[17] Z. Huang *et al.*, "A computer-aided diagnosis system for brain magnetic resonance imaging images using a novel differential feature neural network," *Comput. Biol. Med.*, vol. 121, no. 103818, p. 103818, 2020.

[18] L. Kapoor and S. Thakur, “A survey on brain tumor detection using image processing techniques,” in *2017 7th International Conference on Cloud Computing, Data Science & Engineering - Confluence*, 2017.

[19] L. Zeinalkhani, A. Ali Jamaat, and K. Rostami, “Diagnosis of brain tumor using combination of K-means clustering and genetic algorithm,” *Iran J Med Inform*, vol. 7, p. 6, 2018.

[20] A. Zotin, Y. Hamad, K. Simonov, and M. Kurako, “Lung boundary detection for chest X-ray images classification based on GLCM and probabilistic neural networks,” *Procedia Comput. Sci.*, vol. 159, pp. 1439–1448, 2019.

[21] Uma-E-Hani, S. Naz, and I. A. Hameed, “Automated techniques for brain tumor segmentation and detection: A review study,” in *2017 International Conference on Behavioral, Economic, Socio-cultural Computing (BESC)*, 2017.

[22] Y. A. Hamad, K. Simonov, and M. B. Naeem, “Breast cancer detection and classification using artificial neural networks,” in *2018 1st Annual International Conference on Information and Sciences (AiCIS)*, 2018.

[23] F. A. M. Bargarai, A. M. Abdulazeez, V. M. Tiryaki, and D. Q. Zeebaree, “Management of wireless communication systems using artificial intelligence-based software Defined Radio,” *Int. J. Interact. Mob. Technol.*, vol. 14, no. 13, p. 107, 2020.

[24] D. A. Zebari, D. Q. Zeebaree, A. M. Abdulazeez, H. Haron, and H. N. A. Hamed, “Improved threshold based and trainable fully automated segmentation for breast cancer boundary and pectoral muscle in mammogram images,” *IEEE Access*, vol. 8, pp. 203097–203116, 2020.

[25] A. Bal, M. Banerjee, P. Sharma, and M. Maitra, "Brain tumor segmentation on MR image using K-means and fuzzy-possibilistic clustering," in *2018 2nd International Conference on Electronics, Materials Engineering & Nano-Technology (IEMENTech)*, 2018.

[26] N. A. Zebari, D. A. Zebari, D. Q. Zeebaree, and J. N. Saeed, "Significant features for steganography techniques using deoxyribonucleic acid: A review," *Indonesian Journal of Electrical Engineering and Computer Science*, vol. 21, no. 1, pp. 338–347, 2021.

[27] R. Preetha and S. V. Jinny, "RETRACTED ARTICLE: Early diagnose breast cancer with PCA-LDA based FER and neuro-fuzzy classification system," *J. Ambient Intell. Humaniz. Comput.*, vol. 12, no. 7, pp. 7195–7204, 2021.

[28] M. Faris, T. Javid, K. Fatima, M. Azhar, and R. Kamran, "Detection of tumor region in MR image through fusion of Dam construction and K-mean clustering algorithms," in *2019 2nd International Conference on Computing, Mathematics and Engineering Technologies (iCoMET)*, 2019.

[29] G. Singh and M. A. Ansari, "Efficient detection of brain tumor from MRIs using K-means segmentation and normalized histogram," in *2016 1st India International Conference on Information Processing (IICIP)*, 2016.

[30] C. Saha and M. F. Hossain, "MRI brain tumor images classification using K-means clustering, NSCT and SVM," in *2017 4th IEEE Uttar Pradesh Section International Conference on Electrical, Computer and Electronics (UPCON)*, 2017.

[31] S. Parmar and N. Gondaliya, "A Survey on Detection and Classi ication of Brain Tumor from MRI Brain Images using Image Processing Techniques," *International Research Journal of Engineering and Technology. IRJET*, 2018.

[32] M. Havaei, H. Larochelle, P. Poulin, and P.-M. Jodoin, “Within-brain classification for brain tumor segmentation,” *Int. J. Comput. Assist. Radiol. Surg.*, vol. 11, no. 5, pp. 777–788, 2016.

[33] R. P. Joseph, C. S. Singh, and M. Manikandan, “Brain tumor MRI image segmentation and detection in image processing,” *International Journal of Research in Engineering and Technology*, vol. 3, no. 1, pp. 1–5, 2014.

[34] P. Viola and W. M. Wells, “Alignment by maximization of mutual information,” in *Proceedings of IEEE International Conference on Computer Vision*, 2002.

[35] A. F. Jahwar and A. M. Abdulazeez, “Meta-heuristic algorithms for K-means clustering: A review,” *PalArch’s Journal of Archaeology of Egypt/Egyptology*, vol. 17, no. 7, pp. 12002–12020, 2020.

[36] V. V. P. Wibowo, Z. Rustam, and J. Pandelaki, “Classification of Brain Tumor Using K-Nearest Neighbor-Genetic Algorithm and Support Vector Machine-Genetic Algorithm Methods,” in *2021 International Conference on Decision Aid Sciences and Application (DASA)*, IEEE, 2021, pp. 1077–1081.

[37] S. Modgil and B. Kaur, *Lung Cancer Detection Using CT Images and Various Image Processing Techniques: A*. 2019.

[38] G. Mohan and M. M. Subashini, “MRI based medical image analysis: Survey on brain tumor grade classification,” *Biomed. Signal Process. Control*, vol. 39, pp. 139–161, 2018.

[39] M. Singh, V. Garg, and P. Bhat, “Early Detection of Stroke using Texture Analysis,” *Indian j. forensic med. toxicol.*, vol. 13, no. 3, p. 49, 2019.

[40] C. Zhang, X. Shen, H. Cheng, and Q. Qian, “Brain tumor segmentation based on hybrid clustering and morphological operations,” *Int. J. Biomed. Imaging*, vol. 2019, p. 7305832, 2019.

[41] M. A. A. Mahmud, A. Z. Karim, M. S. Miah, Y. Kim, J. Kim, and S. S. Bashar, "Biomedical Image Processing: Spine Tumor Detection from MRI image using MATLAB," *jcc*, vol. 2, no. 2, pp. 225–235, 2020.

[42] V. K. Lakshmi, C. A. Feroz, and J. A. J. Merlin, "Automated detection and segmentation of brain tumor using genetic algorithm," in *2018 International Conference on Smart Systems and Inventive Technology (ICSSIT)*, IEEE, 2018, pp. 583–589.

[43] M. Vaidyanathan, R. Velthuizen, L. P. Clarke, and L. O. Hall, "Quantitation of brain tumor in MRI for treatment planning," in *Proceedings of 16th Annual International Conference of the IEEE Engineering in Medicine and Biology Society*, 2002.

[44] M. N. Tahir, *Classification and characterization of brain tumor MRI by using gray scaled segmentation and DNN*. 2018.

[45] A. Safonova *et al.*, "Individual tree crown delineation for the species classification and assessment of vital status of forest stands from UAV images," *Drones*, vol. 5, no. 3, p. 77, 2021.

[46] R. O. Silfina, R. Indrati, and L. R. W. Utami, "The role T1-weighted fluid attenuated inversion recovery (FLAIR) post contrast enhancement to improve image quality on MRI brain," *J. Phys. Conf. Ser.*, vol. 1943, no. 1, p. 012052, 2021.

[47] Y. A. Hamad, K. V. Simonov, and M. B. Naeem, "Detection of brain tumor in MRI images, using a combination of fuzzy C-means and thresholding," *Int. J. Adv. Pervasive Ubiquitous Comput.*, vol. 11, no. 1, pp. 45–60, 2019.

[48] B. Tahir *et al.*, "Feature enhancement framework for brain tumor segmentation and classification," *Microsc. Res. Tech.*, vol. 82, no. 6, pp. 803–811, 2019.

[49] V. Rajinikanth and S. C. Satapathy, “Segmentation of ischemic stroke lesion in brain MRI based on social group optimization and fuzzy-Tsallis entropy,” *Arab. J. Sci. Eng.*, vol. 43, no. 8, pp. 4365–4378, 2018.

[50] T. Van Pham and T. T. Tran, “Brain tumor segmentation based on u-Net with image driven level set loss,” *Vietnam J. Sci. Technol.*, vol. 59, no. 5, 2021.

[51] S. Akbar, S. Nasim, S. Wasi, and S. M. U. Zafar, “Image analysis for MRI based brain tumor detection,” in *2019 4th International Conference on Emerging Trends in Engineering, Sciences and Technology (ICEEST)*, 2019.

[52] H. P. A. Tjahyaningtijas, “Brain tumor image segmentation in MRI image,” in *IOP Conference series: materials science and engineering*, vol. 336, IOP Publishing, 2018.

[53] T. Kalaiselvi and S. Karthigai Selvi, “Investigation of image processing techniques in MRI based medical image analysis methods and validation metrics for brain tumor,” *Curr. Med. Imaging Rev.*, vol. 14, no. 4, pp. 489–505, 2018.

[54] K. Yepuganti, S. Saladi, and C. V. Narasimhulu, “Segmentation of tumor using PCA based modified fuzzy C means algorithms on MR brain images,” *Int. J. Imaging Syst. Technol.*, vol. 30, no. 4, pp. 1337–1345, 2020.

[55] B. Thamaraichelvi, “Modified fuzzy clustering-based segmentation through histogram combined with K-NN classification,” *Int. J. Med. Eng. Inform.*, vol. 13, no. 5, p. 410, 2021.

[56] K. Das and A. Das, “Segmentation of brain tumor using cluster validity index-based fuzzy C-means algorithm,” in *Lecture Notes in Bioengineering*, Singapore: Springer Singapore, 2021, pp. 45–56.

[57] G. Latif, J. Alghazo, F. N. Sibai, D. N. F. A. Iskandar, and A. H. Khan, "Recent advancements in Fuzzy C-means based techniques for brain MRI segmentation," *Curr. Med. Imaging Rev.*, vol. 17, no. 8, pp. 917–930, 2021.

[58] B. Biswas, H. S. Soroardi, and M. J. Islam, "Brain tumor detection with tumor region analysis using adaptive thresholding and morphological operation," in *2018 4th International Conference on Electrical Engineering and Information & Communication Technology (iCEEiCT)*, 2018.

[59] E. Mohammed, M. Hassaan, S. Amin, and H. M. Ebied, "Brain tumor segmentation: A comparative analysis," in *Proceedings of the International Conference on Artificial Intelligence and Computer Vision (AICV2021)*, Cham: Springer International Publishing, 2021, pp. 505–514.

[60] M. Sujan, N. Alam, S. Abdullah, and M. Jahirul, "A segmentation based automated system for brain tumor detection," *Int. J. Comput. Appl.*, vol. 153, no. 10, pp. 41–49, 2016.

[61] Y. A. Hamad, K. Simonov, and M. B. Naeem, "Brain's tumor edge detection on low contrast medical images," in *2018 1st Annual International Conference on Information and Sciences (AiCIS)*, 2018.

[62] J. Cheng *et al.*, "Enhanced performance of brain tumor classification via tumor region augmentation and partition," *PLoS One*, vol. 10, no. 10, p. e0140381, 2015.

[63] Y. A. Hamad, K. Simonov, and M. B. Naeem, "Lung boundary detection and classification in chest X-rays images based on neural network," in *Communications in Computer and Information Science*, Cham: Springer International Publishing, 2020, pp. 3–16.

[64] K. He, X. Zhang, S. Ren, and J. Sun, "Deep residual learning for image recognition," in *2016 IEEE Conference on Computer Vision and Pattern Recognition (CVPR)*, 2016.

[65] S. S. Gawande and V. Mendre, “Brain tumor diagnosis using deep neural network (dnn),” *International Journal of Advanced Research in Electrical, Electronics and Instrumentation Engineering*, vol. 5, no. 5, pp. 10196–10203, 2017.

[66] M. K. Islam, M. S. Ali, A. A. Das, D. U. S. Duranta, and M. Alam, “Human brain tumor detection using k-means segmentation and improved support vector machine,” *International Journal of Scientific Engineering Research*, vol. 11, no. 6, 2020.

[67] M. Nasor and W. Obaid, “Detection and localization of early-stage multiple brain tumors using a hybrid technique of patch-based processing, k-means clustering and object counting,” *Int. J. Biomed. Imaging*, vol. 2020, p. 9035096, 2020.

[68] I. Mehidi, D. E. Chouaib Belkhiat, and D. Jabri, “An improved clustering method based on K-means algorithm for MRI brain tumor segmentation,” in *2019 6th International Conference on Image and Signal Processing and their Applications (ISPA)*, 2019.

[69] A. Safonova, Y. Hamad, A. Alekhina, and D. Kaplun, “Detection of Norway spruce trees (Picea Abies) infested by bark beetle in UAV images using YOLOs architectures,” *IEEE Access*, vol. 10, pp. 10384–10392, 2022.

[70] R. Agrawal, M. Sharma, and B. K. Singh, “Segmentation of brain lesions in MRI and CT scan images: A hybrid approach using k-means clustering and image morphology,” *J. Inst. Eng. (India) Ser. B*, vol. 99, no. 2, pp. 173–180, 2018.

[71] S. ShanmugaPriya and A. Valarmathi, “Efficient fuzzy c-means based multilevel image segmentation for brain tumor detection in MR images,” *Des. Autom. Embed. Syst.*, vol. 22, no. 1–2, pp. 81–93, 2018.

[72] A. Zotin, Y. Hamad, K. Simonov, M. Kurako, and A. Kents, “Processing of CT lung images as a part of radiomics,” in *Intelligent Decision Technologies*, Singapore: Springer Singapore, 2020, pp. 243–252.

[73] C. J. J. Sheela and G. Suganthi, "Morphological edge detection and brain tumor segmentation in Magnetic Resonance (MR) images based on region growing and performance evaluation of modified Fuzzy C-Means (FCM) algorithm," *Multimed. Tools Appl.*, vol. 79, no. 25–26, pp. 17483–17496, 2020.

[74] K. Yepuganti, S. Saladi, and C. V. Narasimhulu, "Segmentation of tumor using PCA-based modified fuzzy C means algorithms on MR brain images," *International Journal of Imaging Systems and Technology*, vol. 30, no. 4, pp. 1337–1345, 2020.

[75] M. S. Alam *et al.*, "Automatic human brain tumor detection in MRI image using template-based K means and improved fuzzy C means clustering algorithm," *Big Data Cogn. Comput.*, vol. 3, no. 2, p. 27, 2019.

[76] J. Seetha and S. S. Raja, "Brain tumor classification using Convolutional Neural Networks," *Biomed. Pharmacol. J.*, vol. 11, no. 3, pp. 1457–1461, 2018.

[77] Y. Hamad, O. K. J. Mohammed, and K. Simonov, "Evaluating of tissue germination and growth rate of ROI on implants of electron scanning microscopy images," in *Proceedings of the 9th International Conference on Information Systems and Technologies*, 2019.

[78] Y. A. Hamad, M. E. Seno, M. Al-Kubaisi, and A. N. Safonova, "Segmentation and measurement of lung pathological changes for COVID-19 diagnosis based on computed tomography," *Period. Eng. Nat. Sci. (PEN)*, vol. 9, no. 3, p. 29, 2021.

[79] A. S. Kents, Y. A. Hamad, K. V. Simonov, and A. G. Zotin, "Methods and models for texture analysis of lung pathological changes based on computed tomography for covid-19 diagnosis," *ISPRS - Int. Arch. Photogramm. Remote Sens. Spat. Inf. Sci.*, vol. XLIV-2/W1-2021, pp. 99–105, 2021.

[80] Y. A. Hamad, M. N. Qasim, A. A. Rashid, and M. E. Seno, “Algorithms of experimental medical data analysis,” in *2020 International Conference on Computer Science and Software Engineering (CSASE)*, 2020.

[81] E. Kabaev, Y. Hamad, K. Simonov, and A. Zotin, “Visualization and Analysis of the Shoulder Joint Biomechanics in Postoperative Rehabilitation,” in *SibDATA*, 2020, pp. 34–41.

[82] Y. Hamad, O. K. J. Mohammed, and K. Simonov, “Evaluating of Tissue Germination and Growth Rate of ROI on Implants of Electron Scanning Microscopy Images,” in *Proceedings of the 9th International Conference on Information Systems and Technologies. - 2019*, pp. 1–7.

[83] K. Suzuki, “Overview of deep learning in medical imaging //Radiological physics and technology,” pp. 257–273.

[84] Y. A. Hamad, J. Kadum, A. A. Rashid, A. H. Mohsen, and A. Safonova, “A deep learning model for segmentation of covid-19 infections using CT scans,” in *AIP Conference Proceedings*, vol. 2398, AIP Publishing LLC, 2022.

[85] E. M. Kabaev, Y. A. Hamad, K. V. Simonov, and A. G. Zotin, “METHODS OF INTERPRETATION OF DATA FROM ISOKINETIC TESTS AND MRI STUDIES DURING REHABILITATION OF PATIENTS AFTER RECONSTRUCTIVE SHOULDER JOINT SURGERY. International Archives of the Photogrammetry,” *Remote Sensing & Spatial Information Sciences*, 2021.

[86] A. Zotin, A. Kents, K. Simonov, and Y. Hamad, “Methods of interpretation of CT images with COVID-19 for the formation of feature atlas and assessment of pathological changes in the lungs,” in *Intelligent Decision Technologies*, Singapore: Springer Singapore, 2021, pp. 173–183.

[87] Z. Xiang, H. Tan, and W. Ye, "The excellent properties of a dense grid-based HOG feature on face recognition compared to Gabor and LBP," *IEEE Access*, vol. 6, pp. 29306–29319, 2018.

[88] W. Zhou, S. Gao, L. Zhang, and X. Lou, "Histogram of oriented gradients feature extraction from raw Bayer pattern images," *IEEE Trans. Circuits Syst. II Express Briefs*, vol. 67, no. 5, pp. 946–950, 2020.

[89] K. K. S. Greeshma, *Fashion-MNIST classification based on HOG feature descriptor using SVM," researchgate*. 2019.

[90] E. Kabaev, Y. Hamad, K. Simonov, and A. Zotin, "Visualization and Analysis of the Shoulder Joint Biomechanics in Postoperative Rehabilitation," in *Visualization and Analysis of the Shoulder Joint Biomechanics in Postoperative Rehabilitation*, 2020, pp. 34–41.

[91] D. Konstantinidis, T. Stathaki, V. Argyriou, and N. Grammalidis, "Building detection using enhanced HOG–LBP features and region refinement processes," *IEEE J. Sel. Top. Appl. Earth Obs. Remote Sens.*, vol. 10, no. 3, pp. 888–905, 2017.

[92] J. Yang, Z. Chen, J. Zhang, C. Zhang, Q. Zhou, and J. Yang, "HOG and SVM algorithm based on vehicle model recognition," in *MIPPR 2019: Pattern Recognition and Computer Vision*, 2020.

[93] A. Krishan and D. Mittal, "Multi-class liver cancer diseases classification using CT images," *Comput. J.*, 2021.

[94] H. Hara, T. Hori, K. Sugahara, and H. Yamashita, "Surgical planning of Isshiki type I thyroplasty using an open-source Digital Imaging and Communication in Medicine viewer OsiriX," *Acta Otolaryngol.*, vol. 134, no. 6, pp. 620–625, 2014.

[95] M. Heath, *Current status of the digital database for screening mammography //Digital mammography*. Dordrecht: Springer, 1998.

[96] F. Mohanty, “Digital mammogram classification using 2D-BDWT and GLCM features with FOA-based feature selection approach //Neural Computing and Applications,” pp. 1–15.

[97] A. Kents, Y. Hamad, K. Simonov, A. Zotin, and M. Kurako, “Geometric analysis of pathological changes in lungs using CT images for COVID-19 diagnosis,” in *1st Siberian Scientific Workshop on Data Analysis Technologies with Applications*, SibDATA, 2020, pp. 43–50.

[98] K. Hu *et al.*, “Brain tumor segmentation using multi-cascaded convolutional neural networks and conditional random field,” *IEEE Access*, vol. 7, pp. 92615–92629, 2019.

[99] D. Zhang, G. Huang, Q. Zhang, J. Han, J. Han, and Y. Yu, “Cross-modality deep feature learning for brain tumor segmentation,” *Pattern Recognit.*, vol. 110, no. 107562, p. 107562, 2021.

[100] G. Chen, Q. Li, F. Shi, I. Rekik, and Z. Pan, “RFDCR: Automated brain lesion segmentation using cascaded random forests with dense conditional random fields,” *Neuroimage,* vol. 211, no. 116620, p. 116620, 2020.

[101] W. Wu, “Brain tumor detection and segmentation in a CRF (conditional random fields) framework with pixel-pairwise affinity and superpixel-level features //International journal of computer assisted radiology and surgery,” pp. 241–253.

[102] C. Zhou, C. Ding, X. Wang, Z. Lu, and D. Tao, “One-pass Multi-task networks with cross-task guided attention for brain tumor segmentation,” *IEEE Trans. Image Process.,* vol. 29, pp. 4516–4529, 2020.

[103] R. Ranjbarzadeh, A. Bagherian Kasgari, S. Jafarzadeh Ghoushchi, S. Anari, M. Naseri, and M. Bendechache, “Brain tumor segmentation based on deep learning and an attention mechanism using MRI multi-modalities brain images,” *Sci. Rep.*, vol. 11, no. 1, p. 10930, 2021.

[104] A. Paul, P. Chauhan, H. Sharma, K. Khosla, V. Srivastava, and A. Kumar, “Classification of brain tumor images using enhanced deep learning-based methodologies,” in *Proceedings of International Conference on Data Science and Applications*, Singapore: Springer Singapore, 2022, pp. 519–532.

[105] A. S. Kents, Y. A. Hamad, K. V. Simonov, and A. G. Zotin, “METHODS AND MODELS FOR TEXTURE ANALYSIS OF LUNG PATHOLOGICAL CHANGES BASED ON COMPUTED TOMOGRAPHY FOR COVID-19 DIAGNOSIS. International Archives of the Photogrammetry,” *Remote Sensing & Spatial Information Sciences*, 2021.

[106] D. Zhang *et al.*, “Exploring task structure for brain tumor segmentation from multi-modality MR images,” *IEEE Trans. Image Process.*, vol. PP, pp. 9032–9043, 2020.

[107] M. I. Sharif, M. A. Khan, M. Alhussein, K. Aurangzeb, and M. Raza, “A decision support system for multimodal brain tumor classification using deep learning,” *Complex intell. syst.*, vol. 8, no. 4, pp. 3007–3020, 2022.

[108] F. J. Díaz-Pernas, M. Martínez-Zarzuela, M. Antón-Rodríguez, and D. González-Ortega, “A deep learning approach for brain tumor classification and segmentation using a multiscale convolutional neural network,” *Healthcare (Basel)*, vol. 9, no. 2, p. 153, 2021.